Two Anderson impurities in the Kondo limit: A systematic study of the ground states of the many subspaces of the Hamiltonian

J. Simonin
Centro Atómico Bariloche and Instituto Balseiro, 8400 S.C. de Bariloche, Río Negro, Argentina
(Received 8 March 2005; revised manuscript received 7 February 2006; published 3 April 2006)

We analyze the two-Anderson-impurity problem, in the strong-Coulomb-repulsion limit, by means of variational wave functions whose equations we solve analytically. We found two pairs of doublet states, one odd and one even with respect to the midplane between the impurities. These doublets make a significatively strong use of the hybridization terms of the Hamiltonian and have a much larger Kondo-like correlation energy than a single impurity (the Kondo energy). Furthermore, these doublets combine to form a supersinglet. This supersinglet makes use of the remaining hybridization probability to improve its energy with respect to the doublet energy, but for low-dimensional systems and at the interimpurity distances where the doublets are fully developed, its energy gain is exponentially small. The interaction behind the doublets is a first-order (in the effective Kondo coupling) one; it also generates a parallel alignment of the impurity spins. This ferromagnetic impurity-impurity response is thus generated without resort to the RKKY interaction. The effective range of this first-order Doublet interaction is also much larger than the one of the RKKY interaction.

DOI: 10.1103/PhysRevB.73.155102 PACS number(s): 73.23.−b, 72.15.Qm, 73.63.Kv, 72.10.Fk

I. INTRODUCTION

The two-impurity Anderson (TIA) model is a classic problem in condensed matter physics, where it represents the interaction of two magnetic impurities embedded in a metallic host.[1] The Anderson Hamiltonian is a generic Hamiltonian that describes how localized orbitals with a strong internal Coulomb repulsion behave when they are connected to or through a metallic bath. The current advance in nanotechnology allows for several man-made realizations of such systems:[2,3] quantum dots in the Coulomb blockade regimen connected via a low-dimensional electron gas,[4] magnetic atoms individually deposited on metallic surfaces, nanoclusters or magnetic impurities connected to or through metallic carbon nanotubes, etc. This kind of circuits, characterized by the low dimension of the metallic host, promises to be a relevant circuit component in quantum electronics.

The TIA Hamiltonian has been the subject of many theoretical studies, ranging from perturbation theory[1,5,6] and narrow-band approximation[7] to renormalization group analysis,[8–14] conformal field theory, and quantum Monte Carlo simulations.[15] With some approximations and simplifications, as detailed in Ref. 16, some analytical results have been obtained. Another theoretical approach to Anderson impurity systems has been the use of variational wave functions (VWF's).[17–20] In Ref. 20 a set of VWF equations that describes the lower-energy state of the TIA system has been numerically analyzed. In this paper we present a systematic VWF analysis of the TIA in the strong-Coulomb-repulsion Kondo limit. By means of VWF's we obtain several sets of equations that describe the lower-energy states of different subspaces of the system. We analytically solve those equations, identifying two Kondo-like energy scales[9,13] that depend strongly on the interimpurity distance. The higher one corresponds to the formation of Kondo-like doublet states and the lower one corresponds to the formation of a "composite" Kondo singlet, based upon the screening of the doublet states. Our equations depend on the details of the metallic host through a simple coherence factor that, when needed, we evaluate in the one-dimensional (1D) case because of its importance for technological applications. The 2D and 3D scenarios are also analyzed.

We found that the doublets states generate a ferromagnetic-impurity spin-spin correlation without resort to the RKKY interaction. The effect of the RKKY terms on the doublet structure and energy is also analyzed.

Whereas our analytical results confirm the general picture of the system behavior that is already known from numerical simulations, they also point out that the main interaction between the impurities, contrary to the general belief,[21,22] is not given by the RKKY process but by the simplest electronic process behind the formation of the Kondo-doublet states.

This paper is organized as follows: In Sec. II we write down the TIA Hamiltonian and we make a basis change to the mirror symmetric basis. In Sec. III we make a preliminary study of the system, analyzing the main features of the Hamiltonian at some special distances between the impurities. In Sec. IV we make a systematic analysis of the different subspaces of the Hamiltonian. The effects of the intrinsic RKKY interaction on our states are analyzed in Sec. IV D. The high-dimensional scenarios are analyzed in Sec. V. The impurity spin-spin correlation is evaluated in Sec. VI. In Sec. VII we discuss the conclusions and perspectives open by the method, its possible extension to similar situations, and its relation to previous work.

II. HAMILTONIAN

The Anderson Hamiltonian for magnetic impurities diluted in a metallic host is

 ©2006 The American Physical Society

$$H = \sum_{k\sigma} e_k c^\dagger_{k\sigma} c_{k\sigma} + \frac{V}{\sqrt{N_c}} \sum_{jk\sigma} (e^{i\mathbf{k}\cdot\mathbf{r_j}} d^\dagger_{j\sigma} c_{k\sigma} + \text{H.c.}) - E_d \sum_{j\sigma} d^\dagger_{j\sigma} d_{j\sigma} + U \sum_j d^\dagger_{j\downarrow} d^\dagger_{j\uparrow} d_{j\uparrow} d_{j\downarrow}, \quad (1)$$

where $c_{k\sigma}$ and $d_{j\sigma}$ are fermion operators which act, respectively, on the conduction band states and on the orbital states of the magnetic impurity placed at $\mathbf{r_j}$. Single-state energies $e_k, -E_d$ are referred to the Fermi energy ($E_F = k_F^2/2m$); i.e., there is an implicit $-\mu N$ term in the Hamiltonian that regulates the population of the system ($\mu = E_F$ is the chemical potential and N the total number operator), V is the $d-c$ hybridization, and N_c is the number of cells in the metal. In the Kondo limit that we analyze here the impurity levels are well below the Fermi energy ($-E_d \ll 0$) and cannot be doubly occupied due to the Coulomb repulsion in them ($U \to \infty$). In order to simplify the calculations we renormalize the vacuum (denoted by $|F\rangle$) to be the conduction band filled up to the Fermi energy and we make an electron-hole transformation for band states below the Fermi level: $b^\dagger_{k\sigma} \equiv c_{k\bar{\sigma}}$ for $|k| \leqslant k_F$. In this way the energy of a hole excitation is explicitly positive.

We consider here two impurities placed one at $-\mathbf{r}/2$ (the left impurity) and the other at $\mathbf{r}/2$ (the right impurity).

In this situation ($-E_d < 0$, $U \to \infty$) the lower-energy configurations of the system are the ferromagnetic (FM) triplet $(d^\dagger_{L\uparrow} d^\dagger_{R\uparrow}|F\rangle, \ldots)$ and the antiferromagnetic (AF) singlet $[(d^\dagger_{L\uparrow} d^\dagger_{R\downarrow} - d^\dagger_{L\downarrow} d^\dagger_{R\uparrow})|F\rangle]$, with energies $-2E_d$. These states are not eigenstates of the system because the hybridization term (H_V) mixes these states with configurations having excitations in the band.

An important state for magnetic impurities in a metal is the Kondo singlet, the ground state when a single impurity is considered. If this impurity is at the origin, this singlet is described by the VWF (Ref. 17)

$$|S_o\rangle = |F\rangle - \sum_q Z(q)(b^\dagger_{q\uparrow} d^\dagger_{o\downarrow}|F\rangle + b^\dagger_{q\downarrow} d^\dagger_{o\uparrow}|F\rangle), \quad (2)$$

where the function $Z(q)$ is to be determined variationally. It turns out that $Z(q) = \mathbf{v}/(E_K + E_d - e_q)$. A self-consistent equation is obtained for the singlet energy E_K,

$$E_K = 2\mathbf{v}^2 \sum_q \frac{1}{E_K + E_d - e_q}, \quad (3)$$

where the q sum is over hole excitations ($|q| \leqslant k_F$) and $\mathbf{v} = V/\sqrt{N_c}$. After the form

$$E_K = -E_d - \delta_K \quad (4)$$

is assumed Eq. (3) becomes an equation for the Kondo energy gain δ_K,

$$E_d + \delta_K = 2\mathbf{v}^2 \sum_q \frac{1}{\delta_K + e_q}. \quad (5)$$

From here, in the $E_d, D \gg \delta_K$ regime,

$$\delta_K = D \exp -\frac{1}{2J_n} \quad (6)$$

is obtained. In this equation $J_n \equiv n_o V^2/E_d$, n_o being the density of states at the Fermi level and D the half bandwidth. J_n, the effective Kondo coupling, is the relevant parameter for these systems, and D gives the energy scale. If we demand that δ_K be one thousandth of D, a reasonable value, it follows that $J_n = 0.072\,38$.

Note that although all the $b^\dagger_{q\sigma} d^\dagger_{L\bar{\sigma}}|F\rangle$ configurations enter in the definition of the Kondo singlet, only the holes with $e_q \lesssim \delta_K$ make a significant contribution given that the $Z(q)$ variational amplitude is proportional to $1/(\delta_K + e_q)$. The Fermi state $|F\rangle$ plays the role of a nearly virtual state in the Kondo singlet.

The Hamiltonian, Eq. (1), conserves the total number of electrons, N_T, the total spin S_T, and its projection S_z and has also a mirror symmetry plane at the middle point between the impurities. For example, the FM state has $N_T = 2$ (plus a half-filled conduction band), $S_T, S_z = 1, 1$ and is odd under the mirror reflection ($d^\dagger_{L\uparrow} d^\dagger_{R\uparrow}|F\rangle = -d^\dagger_{R\uparrow} d^\dagger_{L\uparrow}|F\rangle$); the AF state has $N_T = 2$, $S_T = 0$ and is even under reflection. Assuming a canonical ensemble in the thermodynamic limit, this allows the Hamiltonian to be analyzed by subspaces corresponding to different quantum numbers.

It is useful to rewrite the Hamiltonian, Eq. (1), in terms of one-electron operators of well-defined mirror symmetry. This is easily done by changing to the symmetric and antisymmetric combinations

$$c_{Sk\sigma} = \frac{1}{\sqrt{2}}(c_{k\sigma} + c_{\bar{k}\sigma}), \quad c_{Ak\sigma} = \frac{1}{\sqrt{2}}(c_{k\sigma} - c_{\bar{k}\sigma}),$$

$$d_{S\sigma} = \frac{1}{\sqrt{2}}(d_{R\sigma} + d_{L\sigma}), \quad d_{A\sigma} = \frac{1}{\sqrt{2}}(d_{R\sigma} - d_{L\sigma}), \quad (7)$$

where $\bar{k}$ stands for $(-k_x, k_y, k_z)$. The impurities are on the x axis, at $x = \pm r/2$, and the mirror plane is the $x = 0$ plane. The transformed Hamiltonian is

$$H = \sum_{Xk\sigma} e_k c^\dagger_{Xk\sigma} c_{Xk\sigma} - E_d \sum_{X\sigma} d^\dagger_{X\sigma} d_{X\sigma} + 2\mathbf{v} \sum_{k\sigma} \left(\cos \frac{k_x r}{2} d^\dagger_{S\sigma} c_{Sk\sigma} + i \sin \frac{k_x r}{2} d^\dagger_{A\sigma} c_{Ak\sigma} + \text{H.c.} \right), \quad (8)$$

plus eight four-d-operator U Coulomb terms, which can be evaluated when needed. In the Hamiltonian above $X = \{A, S\}$ and the k sum runs only in the right k half-space ($k_x > 0$). The electron-hole transformation for the conduction band states in this basis is just $b^\dagger_{Xk\sigma} \equiv c_{Xk\bar{\sigma}}$ for $|k| \leqslant k_F$.

The effect of the U terms in the $U \to \infty$ limit is to inhibit two of the six two-electron-in-two-impurity states. The forbidden configurations are

$$(d^\dagger_{A\downarrow} d^\dagger_{A\uparrow} + d^\dagger_{S\downarrow} d^\dagger_{S\uparrow})|\,\rangle, \quad (d^\dagger_{A\downarrow} d^\dagger_{S\uparrow} - d^\dagger_{A\uparrow} d^\dagger_{S\downarrow})|\,\rangle, \quad (9)$$

i.e., the symmetric and antisymmetric combinations of the forbidden configurations in the direct basis, $d^\dagger_{L\downarrow} d^\dagger_{L\uparrow}|\rangle$ and

$d^\dagger_{R\downarrow}d^\dagger_{R\uparrow}|\rangle$. The four allowed configurations are

$$|\mathrm{AF}\rangle = (d^\dagger_{A\downarrow}d^\dagger_{A\uparrow} - d^\dagger_{S\downarrow}d^\dagger_{S\uparrow})|\,\rangle, \quad |\mathrm{FM}\uparrow\rangle = d^\dagger_{A\uparrow}d^\dagger_{S\uparrow}|\,\rangle,$$

$$|\mathrm{FM0}\rangle = (d^\dagger_{A\downarrow}d^\dagger_{S\uparrow} + d^\dagger_{A\uparrow}d^\dagger_{S\downarrow})|\,\rangle, \quad |\mathrm{FM}\downarrow\rangle = d^\dagger_{A\downarrow}d^\dagger_{S\downarrow}|\,\rangle, \quad (10)$$

the first one being the AF two-impurity configuration, an even state, the last three being the $S_z=1$, 0, and -1 components of the FM triplet. Higher-impurity-population states are forbidden.

III. MODEL

We base our theory on a careful analysis of the Hamiltonian in the symmetrized basis, Eq. (8). First we notice that in this basis the hybridization terms are decoupled; i.e., symmetric d_S impurity orbitals only mix with symmetric c_S conduction band states and the same is true for the antisymmetric ones. Thus it is appropriate to think in terms of two nearly independent magnetic impurities, the symmetric impurity (SI) and the antisymmetric impurity (AI), keeping in mind that these are linear combinations of the two original impurities. The symmetrized impurities are correlated through the action of the Coulomb interaction because the forbidden impurity occupations are not the doubly occupied SI (or AI) configurations ($d^\dagger_{S\downarrow}d^\dagger_{S\uparrow}|\rangle$ and $d^\dagger_{A\downarrow}d^\dagger_{A\uparrow}|\rangle$) but the combinations thereof given in Eq. (9).

Second, we notice the factor of 2 in the hybridization term of Eq. (8), which originates in the change in the matrix elements of the Hamiltonian due to the change of basis states. This has important consequences because the correlation energy for a magnetic impurity, Eqs. (5) and (6), depends on the effective hybridization raised to the power of 2.

A. Singlet

As a consequence of the above, when the two impurities are at a distance such that $|\cos(k_F r/2)| \simeq 1$ and given that only the conduction holes near the Fermi level are relevant for the formation of a Kondo singlet, the effective coupling for the SI impurity is nearly twice the bare coupling V whereas the effective coupling for the AI impurity is near zero. Therefore, the maximum Kondo-like correlation energy δ_4 that can be obtained by forming a SI Kondo singlet is given by

$$\delta_4 = D \exp -\frac{1}{4J_n}. \quad (11)$$

Notice the factor of 4 in the exponential, while the single-impurity Kondo energy δ_K has only a factor of 2. The effective hybridization coupling provides a 2^2 factor but half the q states in the sum of Eq. (5) have already been summed in doing the basis change, and this is the reason for the change from 2 to 4 in going from δ_K to δ_4. This result is exact for $r=0$ and a good approximation for the next few maxima of the effective SI hybridization coupling ($r \simeq n\lambda_F$, n a small integer, λ_F the Fermi wavelength). This is a very large correlation energy gain for the two-impurity case compared with the single-impurity Kondo energy. For the above given value of $J_n=0.072\,38$ and assuming $D=E_F=10\,000$ K, one obtains $\delta_K=10$ K and $\delta_4=316$ K, a remarkable effect. In fact the δ_4/D ratio is given by the square root of the δ_K/D ratio; thus, this magnification effect is higher the lower δ_K/D.

Let us examine this situation in more detail. Consider first the values of r for which the effective symmetric hybridization coupling is enhanced and the antisymmetric one is depressed, $|\cos(k_F r/2)| \simeq 1, |\sin(k_F r/2)| \simeq 0$—i.e., $r \simeq n\lambda_F$. To analyze these regions we can write down the two-impurity SI singlet $|\mathrm{SI}\rangle$, changing $b^\dagger_{q\sigma}d^\dagger_{L-\sigma}$ by $b^\dagger_{Sq\sigma}d^\dagger_{S-\sigma}$ in the Kondo singlet, Eq. (2). The maximum correlation energy gain for such a state is δ_4; thus, the energy of the SI singlet is $E_{SI} \geqslant -E_d - \delta_4$—i.e., a very high correlation energy gain but a not too low total energy because the average total population of the impurities is 1 for such a state. In Appendix A we show that E_{SI} is always greater than the ground-state energy expected when the two impurities are far apart,

$$E_{2K} = 2E_K = -2E_d - 2\delta_K, \quad (12)$$

the ground-state energy for the two-magnetic-impurity problem in the $r \to \infty$ uncorrelated limit.

B. Doublet

We can try to take advantage of the correlation energy gain δ_4 of the $|\mathrm{SI}\rangle$ singlet by making the SI singlet the core of an odd doublet formed by adding an electron in the inactive AI impurity—i.e., forming the doublet $|D_{o\uparrow}\rangle = d^\dagger_{A\uparrow}|\mathrm{SI}\rangle$. This state has an average total population of two electrons in the impurities but it contains the $d^\dagger_{A\uparrow}d^\dagger_{S\downarrow}|\rangle$ impurity configuration, which is not within the configurations allowed by the U terms of the Hamiltonian, Eqs. (9) and (10). This can be corrected by noting that

$$2d^\dagger_{A\uparrow}d^\dagger_{S\downarrow}|\,\rangle = (d^\dagger_{A\uparrow}d^\dagger_{S\downarrow} + d^\dagger_{A\downarrow}d^\dagger_{S\uparrow})|\,\rangle + (d^\dagger_{A\uparrow}d^\dagger_{S\downarrow} - d^\dagger_{A\downarrow}d^\dagger_{S\uparrow})|\,\rangle. \quad (13)$$

The first combination is the $|\mathrm{FM0}\rangle$ allowed state and the second a forbidden one; thus, we project it out of the wave function. In doing this we are losing 1/4 of the active states of the $|\mathrm{SI}\rangle$ singlet; we will see that this loss reduces the factor of 4 in Eq. (11) to a maximum of 3 for the correlation energy of the doublet. Thus, the odd doublet is given by

$$|D_{o\uparrow}\rangle = d^\dagger_{A\uparrow}|F\rangle + \sum_k S_k\{2Z_1(k)b^\dagger_{Sk\downarrow}|\mathrm{FM}\uparrow\rangle + Z_2(k)b^\dagger_{Sk\uparrow}|\mathrm{FM0}\rangle\}, \quad (14)$$

where $S_k = \cos k_x r/2$. We use the notation of Eq. (10) for the doubly occupied impurity states. We apply the standard analytical Euler-Lagrange minimization procedure to the expectation value of the energy, $E_X = \langle X|H|X\rangle/\langle X|X\rangle$, of this state. For the variational functions in the amplitudes of the wave function components we obtain

$$Z_1(k) = Z_2(k) = \frac{\mathbf{v}}{E_{D_o} + 2E_d - e_k}. \quad (15)$$

We see that they depend on the energy of the doublet E_{D_o}, which is determined by the self-consistent relation

$$E_{D_o} = -E_d + 3\mathbf{v}^2 \sum_q \frac{1+\cos q_x r}{E_{D_o} + 2E_d - e_q}, \tag{16}$$

where the sum index runs over the symmetric hole states—i.e., $|q| \leqslant k_F$ and $q_x \geqslant 0$. As we are looking for the lowest-energy solution of this equation, we assume $E_{D_o} = -2E_d - \delta_o$. Equation (16) becomes a self-consistent equation for δ_o,

$$E_d + \delta_o = 3\mathbf{v}^2 \sum_q \frac{1+\cos q_x r}{\delta_o + e_q}. \tag{17}$$

Two limits can be immediately obtained by just comparing this equation with the self-consistent equation for δ_K, Eq. (5). At $r=0$ one has $\cos q_x r = 1$ for all q's, and thus

$$\delta_3 = \delta_o(r=0) = D \exp -\frac{1}{3J_n}. \tag{18}$$

This is still a great enhancement. For the values used in the previous analysis we obtain $\delta_3 = 100$ K (whereas $\delta_K = 10$ K). This is an exact result because the AI impurity is strictly inactive for $r=0$, this result having been previously found in Ref. 20. For $r \gg 0$ the contribution from the $\cos q_x r$ term in the sum vanishes by decoherence effects; therefore, $\delta_o(r \gg 0) = D \exp\left[-1/\left(\frac{3}{2}J_n\right)\right] \ll \delta_K$. This is a physically wrong result; one expects $\delta_o = \delta_K$ in this limit, but by the same decoherence effects the AI impurity is active in this limit even if $r = M\lambda_F$, M being a very big integer, and its contribution to the odd doublet can no longer be ignored. We correct this point in Sec. IV A.

For the values of r other than the analyzed limits, we must evaluate the sums in Eq. (17). The first one is the Kondo integral

$$I_K(\delta) = \frac{2}{n_o N_c} \sum_q \frac{1}{\delta + e_q} = \ln\left(\frac{D+\delta}{\delta}\right), \tag{19}$$

and the second one can also be summed analytically. We call it the quantum coherence integral, and in 1D we obtain

$$I_Q(\delta, r) = \frac{2}{n_o N_c} \sum_q \frac{\cos q_x r}{\delta + e_q} = \cos(\rho\chi)\left[\mathrm{Ci}(\rho\chi) - \mathrm{Ci}\left(\frac{\rho\delta}{D}\right)\right] + \sin(\rho\chi)\left[\mathrm{Si}(\rho\chi) - \mathrm{Si}\left(\frac{\rho\delta}{D}\right)\right], \tag{20}$$

where $\rho = k_F r$, $\chi = \frac{D+\delta}{D}$, and Ci (Si) is the cosine integral (sine integral) function, as defined in Mathematica. The quantum coherence integral has a logarithmic dependence on δ that goes like I_K. Notice that $I_Q(\delta, 0) = I_K(\delta)$, so it is useful to define the two-impurity coherence factor $C_Q(\delta, r) = I_Q(\delta, r)/I_K(\delta)$, which is a decaying oscillatory function that depends weakly on δ. In Fig. 1 we plot C_Q as a function of r for various values of δ; the r dependence of the 1D-RKKY interaction, $J_R(r)$, is also plotted for comparison. It can be seen that $J_R(r)$ decays rather rapidly, with range $r \simeq \lambda_F$, whereas C_Q has the much larger range ξ_K ($\equiv \lambda_F E_F/\delta_K$), the Kondo length. In 1D the dominant decoherence effect is that of the energy width (δ) of the packet of holes that forms the Kondo cloud. In higher dimensions also angular effects appear that contribute to the decoherence with typical length of the order of λ_F.

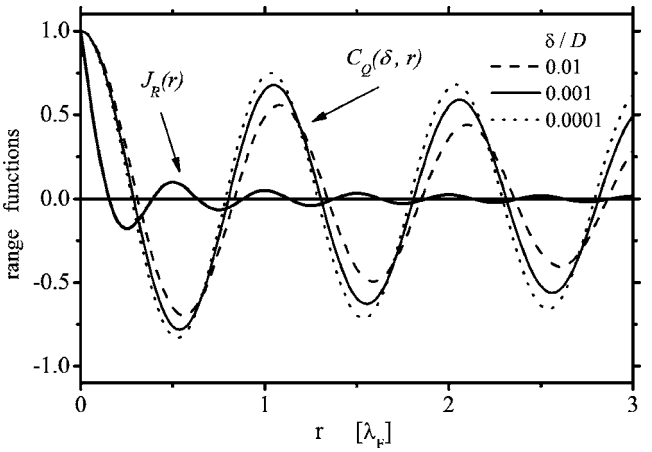

FIG. 1. The two-impurity 1D coherence factor $C_Q(\delta, r)$ and the r dependence $J_R(r)$ of the RKKY interaction as a function of r. Note that C_Q depends weakly on δ. The period of $J_R(r)$ is half the one of C_Q, and its amplitude decays rather rapidly. These characteristics are due to the fact that the RKKY interaction depends on two excitations, whereas the coherence factor involves just one.

Using the results of the sums, Eqs. (19) and (20), Eq. (17) reads

$$E_d + \delta_o = V^2 n_o \frac{3}{2}[1 + C_Q(\delta_o, r)] \ln \frac{D+\delta_o}{\delta_o}, \tag{21}$$

which can be recast as

$$\delta_o(r) = D \exp -\frac{1}{\frac{3}{2}[1 + C_Q(\delta_o, r)] J_n}, \tag{22}$$

still a self-consistent equation, but given the weak dependence of C_Q on δ, it converges very rapidly when used iteratively. It can be easily checked that it gives the two limits already discussed, corresponding to $C_Q = 1$ ($r \to 0$) and $C_Q = 0$ ($r \to \infty$). We will show later, by evaluating the energy of the full odd doublet, that this approximation is in fact good enough at $r \simeq n\lambda_F$, more precisely around the maxima of C_Q. At $r \simeq (n+1/2)\lambda_F$ the more active impurity is the AI one. Therefore for these points we could repeat all the arguments of this section, but for an even doublet based on the AI singlet, however, it is enough to observe that the square of the effective hybridization coupling of the AI impurity goes as $\sin(k_x r/2)^2 \propto [1 - \cos(k_x r)]$. The final result for the correlation energy gain of the even doublet is in fact Eq. (22) but with a minus sign in front of C_Q. We show these energies in Fig. 2 as a function of r. We see that between two consecutive maxima of each of them there is a flat region in which the other one has a maximum. This coincides with the behavior of $[1 \pm C_Q(r)]$ exponentially amplified. Also when δ_o is at one maximum δ_e is very small and vice versa; for the first maxima, their ratio is exponentially small.

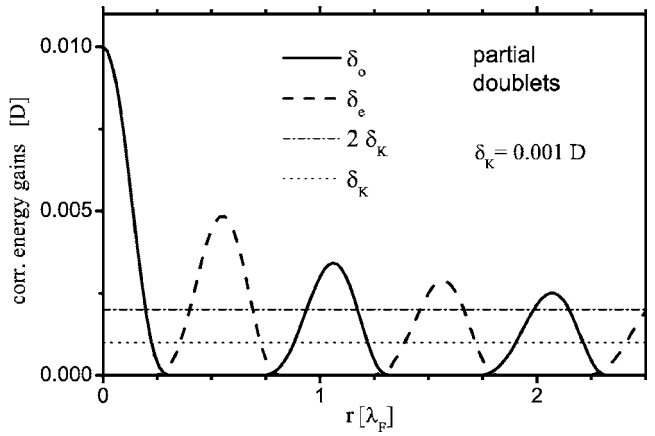

FIG. 2. Correlation energy gains of the odd δ_o and even δ_e doublets as a function of the distance between the impurities, for $J_n=0.072\,38$ ($\delta_K=0.001D$).

From Eqs. (17) and (22) and its equivalent for the even doublet, one can say that $[1+C_Q(\delta_D,r)]/2$ determines the relative strength of the square of the SI impurity hybridization as function of r better than $\cos(k_F r/2)^2$. In fact $C_Q(\delta_D,r)$ has embodied in it the r decoherent effects on the packet of the $n_o\delta_D$ relevant holes of this two-impurity Kondo-like interaction.

C. Supersinglet

At this point of our analysis we see that the odd doublet seems to obtain all the Kondo-like correlation energy of the SI impurity. This is because it is formed out of the ground state of the SI impurity. Furthermore, this doublet, at $r=0$, is probably the ground state of the system, given that coherence effects are at their maximum and the AI hybridization is strictly zero. Furthermore, when δ_o is at one of its maxima, there is very little energy to be gained from the AI impurity, as we can see from the value of δ_e at those same points. Thus it seems that it makes little sense to modify further the structure of these doublets.

However, we see that the vertex state of the $|D_{o\uparrow}\rangle$ doublet is the $d^\dagger_{A\uparrow}|F\rangle$ configuration and $d^\dagger_{A\downarrow}|F\rangle$, the one corresponding to the $S_z=-1/2$ component of the doublet. These states are the ones that can be connected through an AI singlet. Therefore we try the following supersinglet:

$$|SS\rangle = |F\rangle - i\sum_k Z(k)A_k(b^\dagger_{Ak\downarrow}d^\dagger_{A\uparrow} + b^\dagger_{Ak\uparrow}d^\dagger_{A\downarrow})|F\rangle - i\sum_{k,q} Y(k,q)A_kS_q\{(b^\dagger_{Ak\downarrow}b^\dagger_{Sq\uparrow} + b^\dagger_{Ak\uparrow}b^\dagger_{Sq\downarrow})|\mathrm{FM0}\rangle + 2b^\dagger_{Ak\downarrow}b^\dagger_{Sq\downarrow}|\mathrm{FM}\uparrow\rangle + 2b^\dagger_{Ak\uparrow}b^\dagger_{Sq\uparrow}|\mathrm{FM}\downarrow\rangle\}, \quad (23)$$

where $A_k=\sin k_x r/2$. The variational amplitudes $Z(k)$ and $Y(k,q)$ and the supersinglet energy E_S turn out to be

$$Y(k,q) = \mathbf{v}Z(k)/(E_S + 2E_d - e_k - e_q), \quad (24)$$

$$Z(k) = 2\mathbf{v}/D_z(k), \quad (25)$$

$$E_S = 2\mathbf{v}\sum_k [1-\cos(k_x r)]Z(k), \quad (26)$$

where the denominator of $Z(k)$ is

$$D_z(k) = E_S + E_d - e_k - 3\mathbf{v}^2\sum_q \frac{1+\cos q_x r}{E_S + 2E_d - e_k - e_q}.$$

To find E_S we must transform this denominator. It closely resembles Eq. (16) for E_{D_o}, with the change $E_{D_o}\mapsto E_S - e_k$. In fact $D_z(k)$ comes from the contribution of the odd doublet to the $|SS\rangle$ energy. Therefore we assume

$$E_S = E_{D_o} - \gamma = -2E_d - \delta_o - \gamma. \quad (27)$$

Thus, using $\{I_K, I_Q, C_Q\}$ for the sums in D_z and then Eq. (21) for $E_d+\delta_o$, $-D_z(k)$ becomes

$$-D_z(k) = (\gamma + e_k) + \frac{3}{2}V^2 n_o[1 + C_Q(\delta_o,r)]\ln\frac{\delta_o + \gamma + e_k}{\delta_o}; \quad (28)$$

now, note that if $\gamma>0$ [i.e., $E_S<E_{D_o}$], $-D_z(k)$ is always positive. Furthermore, we expect this reduced version of the supersinglet to be good just in the regions in which the odd doublet is. In those regions the contribution to be expected from the AI hybridization channel is very small—i.e., $\delta_o \gg \gamma$—and thus the holes that will contribute the most to the sum in the E_S equation (26) are the ones at an energy distance of the order of γ from the Fermi level. In these conditions the argument of the logarithm in Eq. (28) is very close to 1, and thus it is safe to take $-D_z(k)=(\gamma+e_k)$ when used in the sum of Eq. (26). The next-order correction $[\ln(1+x)\simeq x]$ can be included at no mathematical cost, but it requires introducing a new parameter, the E_d/D ratio. We keep it simple, just disregarding this correction. Therefore, Eq. (26) becomes

$$2E_d + \delta_o + \gamma = 4\mathbf{v}^2\sum_k \frac{[1-\cos(k_x r)]}{\gamma + e_k} = 2V^2 n_o[1 - C_Q(\gamma,r)]\ln\frac{D+\gamma}{\gamma}, \quad (29)$$

from which

$$\gamma(r) = D\exp -\frac{1}{[1-C_Q(\gamma,r)]J_n}. \quad (30)$$

This is a very small number when $\delta_o(r)$ is strong (C_Q near 1). Notice that the C_Q factor in Eq. (30) depends on γ, not on δ_o; thus, it is closer to 1 than $C_Q(\delta_o)$.

Near the second maximum of δ_o, at $r=1.1\lambda_F$, and for $J_n=0.072\,38$, Eq. (22) converges in five iterations to $\delta_o=0.003\,24$ (and $C_Q=0.607$) starting with $\delta_o=\delta_K$ as iteration seed. Equation (30) converges in seven iterations to $\gamma=1.394\times10^{-29}$ ($C_Q=0.792$). Near the first maximum, at $r=0.1\lambda_F$ we obtain $\delta_o=0.009\,22$, $\gamma=5.70\times10^{-124}$.

These are very small numbers indeed, but γ is positive and small enough to justify the approximations made to reduce Eq. (26), and thus the supersinglet is a better option as a possible ground state of the system than the odd doublet.

At $r=0$, $C_Q \equiv 1$ and $\gamma \equiv 0$, and thus, $E_S \equiv E_{D_o}$ and the supersinglet collapses into the odd doublet; i.e., it is an uncorrelated combination of the $b^\dagger_{Ak_F\uparrow}|D_{o\downarrow}\rangle$ and the $b^\dagger_{Ak_F\downarrow}|D_{o\uparrow}\rangle$ states. At $r\to\infty$ ($C_Q=0$) or at the $C_Q(r)=0$ points, this version of the supersinglet fails to give some expected results, mainly that it must be $E_S \simeq -2E_d - 2\delta_K$ for $r\to\infty$. This is not surprising since we already expect this "partial" supersinglet not to give good results outside the $r \simeq n\lambda_F$ regions.

The previous analysis gives us a clear indication of what to look for in the different subspaces of the Hamiltonian, and the chemical potential tells us not to go too far from $N_T=0$ (plus the half-filled conduction band); thus, given the limits that U impose in the population of the impurities, $N_T=2$ seems to be a reasonable upper value. In the next section we proceed to a systematic analysis of those subspaces, looking for the lowest-energy state of each one of them. We start with the $N_T=1$ one and finish with the one corresponding to $N_T=2$. This order is not arbitrary because the $N_T=1$ subspace is the less explored of them and $N_T=2$ the most explored one.

IV. SYSTEMATIC ANALYSIS

A. Doublet subspace, $N_T=1$

The $N_T=1$, odd subspace is the odd doublet subspace. As follows from the previous analysis the odd doublet lacks the action of the AI hybridization channel on its vertex state—i.e., the $b^\dagger_{Ak\uparrow}d^\dagger_{A\downarrow}d^\dagger_{A\uparrow}|F\rangle$ and $b^\dagger_{Ak\downarrow}d^\dagger_{A\uparrow}d^\dagger_{A\uparrow}|F\rangle$ configuration groups. The last group is forbidden by the Pauli exclusion principle and must thus be ignored. For the first group we must use the same procedure as in Eq. (13). Thus we analyze the following variational wave function in this subspace:

$$|D_{o\uparrow}\rangle = d^\dagger_{A\uparrow}|F\rangle + i\sum_k Z_A(k)A_k b^\dagger_{Ak\uparrow}|\mathrm{AF}\rangle + \sum_k Z_S(k)S_k\{2b^\dagger_{Sk\downarrow}|\mathrm{FM}\uparrow\rangle + b^\dagger_{Sk\uparrow}|\mathrm{FM0}\rangle\}, \quad (31)$$

the now full odd doublet. The self-consistent equations for the variational amplitudes and energy are

$$Z_A(k) = Z_S(k) = \frac{\mathbf{v}}{E_{D_o} + 2E_d - e_k}, \quad (32)$$

$$E_{D_o} = -E_d + 2\mathbf{v}^2\sum_q \frac{(3S_q^2 + A_q^2)}{E_{D_o} + 2E_d - e_q}. \quad (33)$$

After expanding the S_q^2 and A_q^2 factors in Eq. (33) and assuming $E_{D_o} = -2E_d - \delta_o$, Eq. (33) transforms into

$$E_d + \delta_o = 2\mathbf{v}^2\sum_q \frac{2+\cos q_x r}{\delta_o + e_q}; \quad (34)$$

now, using $\{I_K(\delta)$, and $C_Q(\delta, r)$, Eqs. (19) and (20)$\}$, Eq. (34) becomes

$$\delta_o(r) = D\exp\frac{-1}{[2 + C_Q(\delta_o, r)]J_n} \quad (35)$$

in the $D, E_d \gg \delta$ limit. This formula for $\delta_o(r)$ replaces the previous partial result, Eq. (22). It can be taken as an approximate solution by evaluating C_Q at δ_K or used iteratively to find the exact result with fast convergency. At its first maxima—i.e., at $\{C_Q \simeq 1, r \simeq n\lambda_F\}$—$\delta_o \leqslant \delta_3$ as previously analyzed. At the $C_Q(\delta, r)=0$ points, including the $r\to\infty$ limit, Eq. (35) gives $\delta_o(r_0 / C_Q(r_0)=0) = \delta_K$ ($\equiv \delta_2$), the physically expected result.

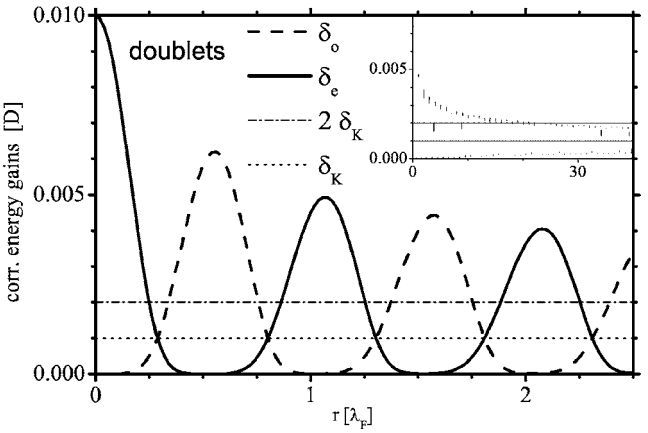

FIG. 3. One-dimensional correlation energy gains of the odd δ_o and even δ_e doublets as a function of the distance between the impurities, for $J_n = 0.072\,38$ ($\delta_K = 0.001D$). The inset is δ_e up to very long distances; it periodically beats $2\delta_K$ up to $r \simeq \xi_K$.

In the $N_T=1$, even subspace, the relevant state being the even doublet, its construction process being the same as for the odd doublet but taking $d^\dagger_{S\uparrow}|F\rangle$ as the vertex state. The definition of the even doublet is similar to that of the odd doublet, Eq. (31), but with the change $A \leftrightarrow S$ in the creation operators and in the hybridization amplitude factors A_k and S_k. A global minus sign appears for the $Z_X(k)$, given that for the AF and FM states we use the $d^\dagger$ operator ordering shown in Eq. (10), the one of the allowed impurity configurations. The energy E_{D_e} of the even doublet states is given by

$$E_{D_e}(r) = -2E_d - \delta_e(r),$$

$$\delta_e(r) = D\exp\frac{-1}{[2 - C_Q(\delta_e, r)]J_n}. \quad (36)$$

If we compare Eq. (36) for $\delta_e(r)$ with Eq. (35) for $\delta_o(r)$, we see that the sign in front of C_Q changes, this being because of the $A_k \leftrightarrow S_k$ change; i.e., the SI and AI impurities interchange roles. The analysis of δ_e as a function of r is also very similar to that of $\delta_o(r)$. The odd-doublet correlation energy gain $\delta_o(r)$ is higher than the even-doublet gain δ_e when $C_Q(\delta_K, r) > 0$, and the opposite is true for $C_Q(\delta_K, r) < 0$. They are equal and equal to $\delta_K = \delta_2$, at the r_K distances for which $C_Q(\delta_K, r_K) = 0$.

These correlation energy gains of the odd and even doublets, δ_o and δ_e, are plotted in Fig. 3 as a function of r for $\delta_K = 0.001D$. For very large r, such that $C_Q(\delta_K, r)$ vanishes, the energy gain of the doublets tends to that of one Kondo singlet. This is not surprising since the doublets, in this limit, can be written as

$$|D_{X\uparrow}\rangle = |L_\uparrow\rangle \otimes |S_R\rangle \pm |S_L\rangle \otimes |R_\uparrow\rangle, \tag{37}$$

i.e., the combination of a Kondo singlet in one of the original impurities and the other single occupied plus (minus) the mirror image of that state. The total energy of this state is $-2E_d-\delta_K$, as for the doublets in the uncorrelated limit ($r\to\infty$).

These energy gains must be compared with twice the Kondo energy, because, for very large r, the latter is the energy gain for a state that has simultaneously and, in a uncorrelated way, both impurities forming a Kondo singlet ($|S_L\rangle\otimes|S_R\rangle$). The doublet gains δ_D alternatively surpass $2\delta_K$ up to $r\simeq\xi_K$.

This effect, $\delta_>=\max(\delta_o,\delta_e)\geqslant 2\delta_K$, is present for values of J_n lower than $J_{n_c}=0.240$ (defined by $\delta_3=2\delta_2$); the lower J_n, the greater this effect. The periodicity with which $|D_o\rangle$ and $|D_e\rangle$ alternate as ground states of the $N_T=1$ subspace is twice the RKKY period [they are ruled by $C_Q(\delta_K)$], and they stand in this situation up to very long distances. These properties are due to the fact that the doublet coherence integral involves just one hole excitation. At the intersection points one has $\delta_e,\delta_o=\delta_K$ and $C_Q=0$.

The electronic process behind these correlated doublets is second order in the hybridization coupling V. The jump of a band electron from below the Fermi level to the impurities and then back to its initial place is the only process allowed by the doublet VWF, Eq. (31).

B. Supersinglet, $N_T=0$

In the $N_T=0$ subspace there is the supersinglet, its full expression, taking into account both the even and odd doublet components, being

$$\begin{aligned}|SS\rangle = |F\rangle &- \sum_k \{[iZ_O(k)A_k(b^\dagger_{Ak\downarrow}d^\dagger_{A\uparrow}+b^\dagger_{Ak\uparrow}d^\dagger_{A\downarrow})\\ &+ Z_E(k)S_k(b^\dagger_{Sk\downarrow}d^\dagger_{S\uparrow}+b^\dagger_{Sk\uparrow}d^\dagger_{S\downarrow})]|F\rangle\}\\ &- \sum_{k,q}\{[Y_O(k,q)A_kA_qb^\dagger_{Ak\downarrow}b^\dagger_{Aq\uparrow}+Y_E(k,q)S_kS_qb^\dagger_{Sk\downarrow}b^\dagger_{Sq\uparrow}]\\ &\times|\mathrm{AF}\rangle + iY(k,q)S_kA_q[(b^\dagger_{Aq\downarrow}b^\dagger_{Sk\uparrow}+b^\dagger_{Aq\uparrow}b^\dagger_{Sk\downarrow})|\mathrm{FM0}\rangle\\ &+ 2b^\dagger_{Aq\downarrow}b^\dagger_{Sk\downarrow}|\mathrm{FM}\uparrow\rangle + 2b^\dagger_{Aq\uparrow}b^\dagger_{Sk\uparrow}|\mathrm{FM}\downarrow\rangle]\}.\end{aligned} \tag{38}$$

The $Z_{O(E)}(k)$ configurations are the odd- (even-) doublet component of the supersinglet. The "origin" of each one of its components can also be traced down looking at the A_k and S_k factors and/or the results obtained for their variational amplitude functions. After the functional minimization procedure, these functions turn out to be

$$\begin{aligned}Y_O(k,q) &= \mathbf{v}[Z_O(k)+Z_O(q)]/D_Y(k,q),\\ Y_E(k,q) &= \mathbf{v}[Z_E(k)+Z_E(q)]/D_Y(k,q),\\ Y(k,q) &= \mathbf{v}[Z_O(k)+Z_E(q)]/D_Y(k,q),\end{aligned} \tag{39}$$

where $D_Y(k,q)=(E_S+2E_d-e_k-e_q)$ and

$$\begin{aligned}Z_O(k) = -\Big[&2\mathbf{v}+\mathbf{v}^2\sum_q(1-\mathrm{cqr})Z_O(q)/D_Y(k,q)\\ &+3\mathbf{v}^2\sum_q(1+\mathrm{cqr})Z_E(q)/D_Y(k,q)\Big]\Big/D_{Z_O}(k),\end{aligned} \tag{40}$$

$$D_{Z_O}(k) = -E_S-E_d+e_k+2\mathbf{v}^2\sum_q\frac{2+\mathrm{cqr}}{D_Y(k,q)}, \tag{41}$$

where $\mathrm{cqr}=\cos q_x r$. For $Z_E(k)$ a symmetric expression holds, with the changes, in Eqs. (40) and (41), $E\leftrightarrow O$, $A\leftrightarrow S$, and $\mathrm{cqr}\mapsto-\mathrm{cqr}$. For the supersinglet energy E_S, the following expression is obtained:

$$E_S = 2\mathbf{v}\sum_k[(1-\mathrm{ckr})Z_O(k)+(1+\mathrm{ckr})Z_E(k)]. \tag{42}$$

To solve these equations, which are self-consistent and recursive, one must proceed in a similar way as in the case of the partial supersinglet analyzed in Sec. III C. We work them out in the same approximation as before, disregarding higher-order terms that depend on the E_d/D ratio.

First, we analyze the points at which coherence effects are suppressed—i.e., $r\to\infty$ and the r_K points such that $C_Q(\delta_K,r_K)=0$. For these points $\delta_o=\delta_e=\delta_K$ and thus, assuming $E_S=-2E_d-\delta_K-\gamma$, we obtain

$$Z_X = -2\mathbf{v}/D_{Z_X}, \tag{43}$$

$$D_{Z_X} = (\gamma+e_k), \tag{44}$$

$$2E_d+\delta_K+\gamma = 8\mathbf{v}^2\sum_k\frac{1}{\gamma+e_k}, \tag{45}$$

from which $\gamma=\delta_K$ follows. Therefore, the energy of the supersinglet at these points is

$$E_S = -2E_d-2\delta_K. \tag{46}$$

The value $C_Q(\delta_K,r_K)=0$ marks the boundary between two regions. For $C_Q(\delta_K,r)>0$ the odd doublet is the lower-energy doublet and it is the main component of the supersinglet; conversely, for $C_Q(\delta_K,r)<0$ the behavior of the supersinglet is determined by the even doublet. We work out now the energy of the supersinglet in the odd-doublet region. In these regions $\delta_o>\delta_e$ and thus we take $E_S=-2E_d-\delta_o-\gamma$. With this replacement Eqs. (40) and (42) become

$$D_{Z_O} = (\gamma+e_k), \quad D_{Z_E} = (\gamma+\Delta_\delta+e_k), \tag{47}$$

$$E_S = -4\mathbf{v}^2\sum_k\left[\frac{1-\mathrm{ckr}}{D_{Z_O}(k)}+\frac{1+\mathrm{ckr}}{D_{Z_E}(k)}\right]. \tag{48}$$

Using the definitions of $\{I_K,I_Q,C_Q\}$ and the proposed form of E_S, Eq. (47) transforms into

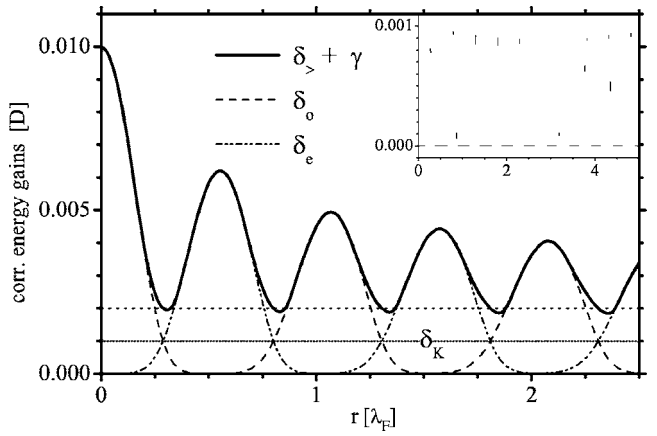

FIG. 4. Correlation energy gains of the odd δ_o and even δ_e doublets and supersinglet $\delta_> + \gamma$ as a function of the distance between the impurities, for $J_n = 0.072\,38$ ($\delta_K = 0.001D$) in the 1D case. The inset is γ, the additional energy gained in forming the supersinglet. For large r it tends to δ_K and the total energy of the supersinglet to $-2E_d - 2\delta_K$.

$$\frac{1}{J_n} = I_K(\gamma)[1 - C_Q(\gamma, r)] + I_K(\gamma + \Delta_\delta)[1 + C_Q(\gamma + \Delta_\delta, r)], \tag{49}$$

from which one obtains

$$\gamma(r) = De^{-1/J_n[1-C_Q(\gamma)]}\left(\frac{D}{\Delta_\delta + \gamma}\right)^{[1+C_Q(\gamma+\Delta_\delta)]/[1-C_Q(\gamma)]}, \tag{50}$$

where $\Delta_\delta = \delta_o - \delta_e$; only the energy dependence of C_Q is shown. This is the full expression for γ when the odd doublet is the dominant one. For $C_Q(\delta_K) = 0$ one has $\delta_o = \delta_e = \delta_K$, and Eq. (50) reduces to $\gamma^2 = D^2 \exp(-1/J_n)$—i.e., $\gamma = \delta_K$; see Eq. (46).

At the maxima of C_Q ($r \simeq n\lambda_F$) one has $\delta_o \gg \delta_e, \gamma$—thus, $\Delta_\delta \simeq \delta_o$—and using Eq. (35) one obtains

$$\gamma = D \exp\left\{-\frac{1}{J_n[1 - C_Q(\gamma)]}\left[1 + \frac{1 + C_Q(\delta_o)}{2 + C_Q(\delta_o)}\right]\right\}, \tag{51}$$

i.e., nearly Eq. (30), the previous "partial" result for γ at those regions. For these maxima, γ is exponentially small if $C_Q(\gamma, r)$ is still strong, as discussed in Sec. III C.

To analyze the r regions in which $C_Q(\delta_K, r) < 0$ one must propose $E_S = -2E_d - \delta_e - \gamma$ given that for these regions $\delta_o < \delta_e$. The result for γ is just Eq. (49) with the changes $\delta_o \leftrightarrow \delta_e$ and $C_Q \rightarrow -C_Q$. In Fig. 4 we plot the correlation energy gains of the doublets and the supersinglet.

At the first maxima of the doublet energy gains—i.e., the minima of their total energy—the additional energy gain of the supersinglet γ is very small and therefore small thermal activation will destroy the correlation that generates it. This is not the case for the energy gain of the doublets at those points, δ_o or δ_e, which is very strong, as discussed in Sec. III B.

C. $N_T = 2$ subspace

In this subspace there are the lower-energy configurations of the system, the AF singlet and the FM triplet, whose configurational energy is $-2E_d$. Given that these configurations are already the lower-energy configurations of the subspace, the effects of the hybridization on them can be directly evaluated by standard perturbation methods. For the sake of completeness we recalculated the result of Ref. 5 in the same variational wave function framework as the previously analyzed subspaces. We use the "perturbation" property of the AF and FM states to solve their self-consistent energy equation by series expansion. For these AF and FM states two hybridization (H_V) steps are needed to bring out the RKKY energy term. For the $S_z = 1$ component of the FM triplet, the expanded VWF is

$$\begin{aligned}
&|\mathrm{FM_{RKKY}}\uparrow\rangle \\
&= |\mathrm{FM}\uparrow\rangle - \sum_k Z(k)(S_k c^\dagger_{Sk\uparrow} d^\dagger_{A\uparrow} + iA_k c^\dagger_{Ak\uparrow} d^\dagger_{S\uparrow})|F\rangle \\
&+ \sum_{k,q} Y(k,q)\{(2A_kA_q b^\dagger_{Ak\downarrow} c^\dagger_{Aq\uparrow} + 2S_kS_q b^\dagger_{Sk\downarrow} c^\dagger_{Sq\uparrow})|\mathrm{FM}\uparrow\rangle \\
&+ (A_kA_q b^\dagger_{Ak\uparrow} c^\dagger_{Aq\uparrow} + S_kS_q b^\dagger_{Sk\uparrow} c^\dagger_{Sq\uparrow})|\mathrm{FM0}\rangle \\
&+ i(S_kA_q b^\dagger_{Sk\uparrow} c^\dagger_{Aq\uparrow} - A_kS_q b^\dagger_{Ak\uparrow} c^\dagger_{Sq\uparrow})|\mathrm{AF}\rangle\}.
\end{aligned} \tag{52}$$

After minimization, it turns out that

$$Y(k,q) = \frac{\mathbf{v}Z(q)}{D_Y(k,q)}, \tag{53}$$

$$Z(k) = \frac{2\mathbf{v}}{D_Z(k)}, \tag{54}$$

$$D_Z(k) = E_{\mathrm{FM}} + E_d - e_k - 2\mathbf{v}^2 \sum_q \frac{2 + \mathrm{cqr\ ckr}}{D_Y(k,q)}, \tag{55}$$

$$E_{\mathrm{FM}} = -2E_d + 2\mathbf{v}\sum_k Z(k), \tag{56}$$

where $D_Y(k,q) = E_{\mathrm{FM}} + 2E_d - e_k - e_q$. As in the previous cases, the energy is to be determined self-consistenly. We can make a Taylor series expansion on $\mathbf{v}^2$ on the right of Eq. (56), taking into account that E_{FM} is also a function of $\mathbf{v}^2$. If this expansion is carefully analyzed, it turns out that the expansion parameter is J_n. The final result for E_{FM}, to order $\mathbf{v}^4$, is the well-known perturbation theory expression

$$\begin{aligned}
E_{\mathrm{FM}} = &-2E_d - \mathbf{v}^2 \sum_k \frac{4}{E_d + e_k} + \mathbf{v}^4 \sum_{k,q} \left\{ \frac{16}{(E_d + e_k)^2 (E_d + e_q)} \right. \\
&\left. - \frac{16 + 8\cos q_x r \cos k_x r}{(E_d + e_k)^2 (e_k + e_q)} \right\},
\end{aligned} \tag{57}$$

the first $\mathbf{v}^4$ term in the right being the second-order contribution of the $\mathbf{v}^2$ correction. This a well-known property of variational wave functions like the Kondo Varma-Yafet singlet. In the second $\mathbf{v}^4$ term there is a contribution that depends on the interimpurity distance r,

$$\Sigma_R(r) \simeq 8\frac{\mathbf{v}^4}{E_d^2}\sum_{kq}\frac{\cos(q_x r)\cos(k_x r)}{(e_k+e_q)} = 4\ln 2 D J_n^2 J_R(r), \tag{58}$$

this being half the RKKY energy. The prefactor of 8 appears because the sum in Eq. (58) is over $k_x>0$ ($q_x>0$) electron (hole) excitations. The r-dependent part $J_R(r)$ of the 1D-RKKY is given by[23]

$$J_R(r) = \frac{2}{\pi}\left[\frac{\pi}{2} - \mathrm{Si}(2k_F r)\right], \tag{59}$$

which is plotted in Fig. 1. It decays very fast, its first extreme values being 1.0 at $r=0.0\lambda_F$ and -0.179 at $\lambda_F/4$. At $r=2.0\lambda_F$ its value 0.025 is already very small. The $r=0$ value of Σ_R is determined by integration of Eq. (58) in the half-filled flatband approximation for the conduction band of the metallic host. The Kondo energy, Eqs. (5) and (6), is also evaluated in that approximation. For the AF state, expanded to the same order as the FM state, there appear the same terms as in Eq. (57) but with a minus sign in front of Σ_R; thus, the RKKY interaction—i.e., the energy difference between the FM and AF states—is twice Σ_R.

D. RKKY and doublet states

The doublet states are the results of a first-order interaction present in the TIA Hamiltonian. Only the configurations that are reached with one H_V step from the corresponding vertex state are included in the VWF's we use to study them. Note also that it depends on J_n (although in a nonperturbative way) and that just one hole excitation is involved in the calculus of C_Q. The RKKY is a second-order interaction, two H_V steps are needed in their VWF, it depends on J_n^2, and both a hole and an electron excitation are involved in its evaluation. In fact, the correlation energy of the dominant doublet is higher than that corresponding to the RKKY in most of the (J_n, r) parameter space of the Hamiltonian. At $r=0$ the equation $\Sigma_R(0)=\delta_3$ determines that for $J_n>0.085$ the doublet correlation energy is greater than the RKKY energy. Note that the one-impurity Kondo energy δ_K is never greater than $\Sigma_R(0)$. As a function of r the RKKY interaction decays at shorter distances than the doublet one. In Fig. 5 we show the "doublet-RKKY" "parameters-space phase diagram" for the 1D two-impurity system, determined by $\max(\delta_o, \delta_e)=|\Sigma_R|$. This is not a true quantum-phase diagram given that neither the doublet nor the FM (AF) states are the ground state of the system. But it indicates the (J_n, r) regions in which the second-order RKKY must be included in the analysis of the doublet structure. Over the near vertical dashed lines that mark the limits between the odd and even doublets, determined by $C_Q(\delta_K)=0$, there is little enhancement of the doublet energies. These zones coincide with the AF maxima of the RKKY interaction and thus over these lines there are the highest indents of the RKKY regions.

How $\Sigma_R(r)$ modifies the internal structure of the doublets has been analyzed in Ref. 24, where the doublets where introduced. To include the RKKY effects in the VWF of the odd doublet, two more H_V generations of configurations must be added to it. In the odd-doublet VWF, Eq. (31), see that the configurations with the $Z_A(k)$ amplitude factor correspond to an AF state of the impurities, whereas the ones with the $Z_S(k)$ factor are configurations with their impurity part in a FM state. As in Sec. IV A we cut our VWF at that order thus both amplitude factors result to be equal, $Z_A=Z_S=\mathbf{v}/[E_{D_o}-(-2E_d+e_k)]=-\mathbf{v}/(\delta_o+e_k)$. We show in Appendix C that the main effect of the configurations needed to include the RKKY interaction in our doublet VWF is to modify those amplitude factors. Their denominators will reflect now the different energies of the FM and AF impurity configurations. The self-consistent equation for the odd-doublet energy when these higher-order processes are included is given by

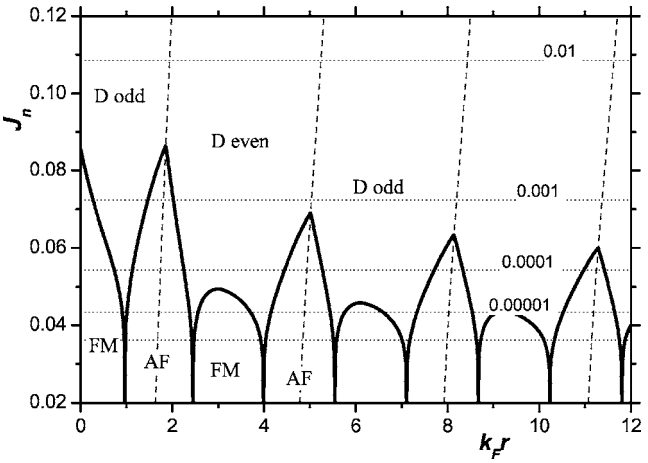

FIG. 5. Doublet-RKKY 1D "quantum phase diagram" for the TIA Hamiltonian. The horizontal dot lines mark the values of δ_K (in units of D) for the corresponding values of J_n.

$$E_D = -E_d + \sum_k \frac{3\mathbf{v}^2[1+\cos(k_x r)]}{E_D + 2E_d + 2\Sigma_0 + \frac{1}{4}J_X + \Sigma_R - e_k} + \sum_k \frac{\mathbf{v}^2[1-\cos(k_x r)]}{E_D + 2E_d + 2\Sigma_0 - \frac{3}{4}J_X - \Sigma_R - e_k}, \tag{60}$$

where the first sum on the right comes from the contribution of the ferromagnetic configurations in the doublet and the second one from the antiferromagnetic configurations, Σ_0 is the one impurity correction (up to second order in J_n), and the terms proportional to J_X appear, just with the VWF used in Sec. IV A, if an external RKKY-like term $(-J_X S_L \cdot S_R)$ is added to the TIA Hamiltonian. The effect of Σ_0 is to shift the "zero" of energy, and the effect of J_X is similar to the one of the intrinsic RKKY term Σ_R; thus, in what follows we discuss just the effects of this last term in the doublet structure and energy. With the considerations above, the variational amplitude factor of the FM configurations in the doublet is given by $Z_S(k)=-\mathbf{v}/(\Delta_o-\Sigma_R+e_k)$ when RKKY effects are taken into account. And for the AF configurations, $Z_A(k)=-\mathbf{v}/(\Delta_o+\Sigma_R+e_k)$ holds. $\Delta_o=|\Sigma_R(r)|+\delta_o^{\Sigma}(r)$ is the total correlation energy gain of the doublet, composed by the RKKY and Kondo-doublet contributions.

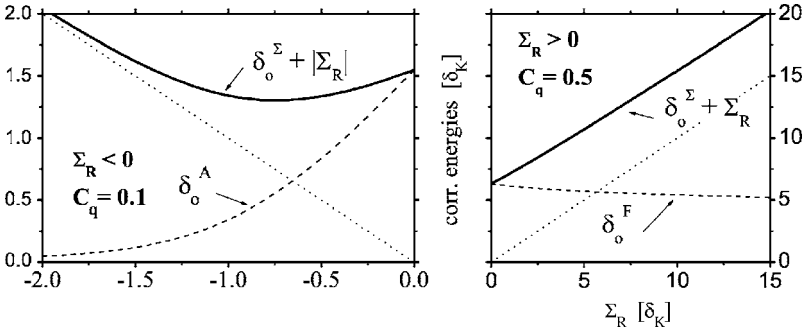

FIG. 6. Correlation energy gain of the odd doublet when a non-negligible RKKY interaction is present. Note the change of scales (and behavior) between the left panel, corresponding to the $\Sigma_R<0$ case, and the right panel, which corresponds to the $\Sigma_R>0$ case.

For $\Sigma_R>0$ (which corresponds also to the maxima of $|C_Q|$), the dominant components of the dominant doublet are the FM configurations; thus, we assume $E_D=-2E_d-\Sigma_R-\delta_o^{\Sigma}$, and using the definitions of I_K and C_Q, we obtain

$$\frac{1}{J_n}=\frac{3[1+C_Q(\delta_o^{\Sigma})]}{2}\ln\frac{D}{\delta_o^{\Sigma}}+\frac{[1-C_Q(\delta_o^{\Sigma}+2\Sigma_R)]}{2}\ln\frac{D}{\delta_o^{\Sigma}+2\Sigma_R}, \tag{61}$$

a self-consistent equation that easily gives the value of the odd-doublet correlation energy (δ_o^{Σ}) in a RKKY-FM region. In the extreme case $\Sigma_R \gg \delta_o$ one can neglect the AF-configuration contributions to Eq. (61) [this is equivalent to using for the doublets a VWF with $Z_A(k)\equiv 0$] and thus

$$\delta_o^{\Sigma}=D\exp\frac{-1}{(3/2)(1+C_Q)J_n}, \tag{62}$$

which gives $\delta_o^{\Sigma}>\delta_K$ for values of $|C_Q|$ down to 1/3. Note also that for high values of C_Q there is little reduction of δ_o^{Σ} compared with its bare ($\Sigma_R=0$) value δ_o, because the AF-configuration contribution [$\sim(1-C_Q)/2$] is already very small in this case.

Similarly, in the RKKY-AF regions ($\Sigma_R<0$ and $C_Q\simeq 0$), we assume $E_D=-2E_d-|\Sigma_R|-\delta_o^{\Sigma}$ and, with the notation $\Sigma_A=|\Sigma_R|=-\Sigma_R$, the general equation (60) can be expressed as

$$\frac{1}{J_n}=\frac{3[1+C_Q(\delta_o^{\Sigma}+2\Sigma_A)]}{2}\ln\frac{D}{\delta_o^{\Sigma}+2\Sigma_A}+\frac{[1-C_Q(\delta_o^{\Sigma})]}{2}\ln\frac{D}{\delta_o^{\Sigma}}, \tag{63}$$

which in the extreme case $\Sigma_A \gg \delta_K$ can be reduced to

$$\delta_o^{\Sigma}=D\exp\frac{-1}{(1/2)(1-C_Q)J_n}, \tag{64}$$

which gives very small values for the correlation energy of the doublet in this situation: for $J_n=0.072\,38$, which corresponds to $\delta_k=0.001D$ and $\delta_3=\delta_o(r=0)=0.01D$, one obtains $\delta_o^{\Sigma}=0.000\,000\,000\,001D$. Therefore the formation of the doublets in an extreme RKKY-AF region will be very difficult to detect in a numerical simulation of the system. Experimentally, nearly any thermal activity will destroy the doublets in this regime.

The previous equations [Eqs. (60)–(64)] are for the odd doublet, which dominates for $C_Q>0$. As the equations corresponding to the even doublet (which dominates for $C_Q<0$) are the same but with a minus in front of C_Q; the final result is that Eqs. (61)–(64) also apply to the even doublet with the change $C_Q\rightarrow -C_Q$. In Fig. 6 we show a "generic" analysis of Eq. (60): for $J_n=0.072\,38$ and fixed values of C_Q we plot δ_o^{Σ} as a function of Σ_R ($-\Sigma_R$) on the right (left) panel, energies being in units of δ_K. Actually, both C_Q and Σ_R are precise functions of (J_n,r) and not any value of Σ_R can be obtained for a given J_n. Anyway, we use this figure to show the general trend of the solutions of Eq. (60). It can be seen that a positive Σ_R has little effect on the dominant doublet structure, and it nearly has just an additive effect on the total energy of the doublet. This response is due to the fact that the dominant doublet is primarily formed upon FM-like configurations. By the same reason a negative Σ_R, which energetically penalizes the FM-like configurations, has a catastrophic effect on the energy gained by forming the doublet. The corresponding extreme limits are well described by Eqs. (62) and (64).

In Fig. 7 we plot the total correlation energy of the doublets ($\Delta_x=\delta_x^{\Sigma}+|\Sigma_R|$, $x=\{o,e\}$) as a function of the distance between the impurities and for $J_n=0.072\,38$. As discussed previously the main contribution to the energy of the dominant doublet comes from the Kondo-doublet interaction, the RKKY contribution becoming negligible very rapidly when the distance between the impurities is increased beyond $\lambda_F/2$. For the dominated doublet, instead, nearly all the en-

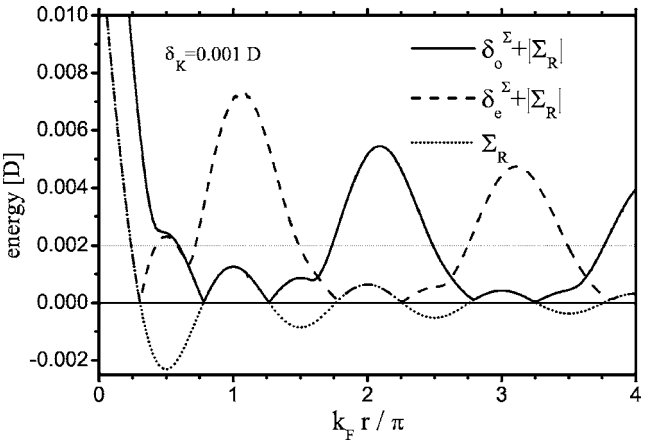

FIG. 7. Correlation energy of the doublets including RKKY effects, for $J_n=0.072\,38$ and as a function of the interimpurity distance r. The dominant doublet energy is mainly composed by the Kondo-doublet energy. Only at $k_F r=\pi/2$ is the correlation energy nearly fully provided by the RKKY interaction. This point corresponds to a maximum of the RKKY-AF energy and a zero of C_Q.

ergy gain comes from the RKKY contribution. Only at $k_F r = \pi/2$, a crossing point for the doublets ($C_Q=0$), does the RKKY-AF interaction provide "all" the energy gain of the dominant doublet. This point is an extreme RKKY-AF case, as described by Eq. (64).

These extreme RKKY-AF regions, which for the actual TIA Hamiltonian are only present for low values of J_n, are the subject of contradictory results in the literature. Numerical renormalization group (NRG) calculations seem to support a crossover from a Kondo-singlet to an AF-singlet for these regions. Instead, quantum Monte Carlo[15] and numerical VWF (Ref. 18) calculations do not give support for such a quantum phase transition to occur in the $U\rightarrow\infty$ limit of the TIA Hamiltonian. Our analytical VWF analysis is in line with these latter results for these extreme RKKY-AF cases: although with a very low correlation energy the Kondo doublets are formed on top of the AF configurations. Note that this result only applies in the analyzed limit of the TIA Hamiltonian and assuming that the RKKY-AF effects can be analyzed in a perturbative way. We have used this last property to obtain the standard RKKY result in Sec. IV C and also in Appendix C to obtain Eq. (60). Note also that in this limit one has $|Z_A(k)| \gg |Z_S(k)|$ $[1/(\delta_o^{\Sigma}+e_k) \gg 1/(\delta_o^{\Sigma}+2|\Sigma_R| + e_k)]$ and thus the properties of the doublet are determined mainly by its AF group of configurations.

We have restricted our previous analysis to scenarios that are actually present in the analyzed limit of the TIA Hamiltonian: ferromagnetic RKKY regions coincide with the maxima of $|C_Q(r)|$ and antiferromagnetic RKKY regions are in correspondence with $C_Q(r)\simeq 0$. If one takes C_Q and Σ_R as free parameters, as is often done in NRG simulations using the Kondo Hamiltonian, one can achieve the following situation: a strong AF RKKY and $C_Q=1$. In this case the self-consistent solution of Eq. (64) gives $\delta_o^{\Sigma}\equiv 0$ and the doublet is not formed. This is a possible explanation for the contradictory numerical results present in the literature.

V. C_Q IN THE 2D AND 3D SCENARIOS

In the previous sections, when needed for graphical purposes and because of its technological applications, we have evaluated our equations in the 1D case. In 1D the only decoherence factor, both for C_Q and the RKKY interaction, is the energy width of the packet of excitations involved in the interaction. In higher dimensions the angular decoherence effect dominates the behavior of C_Q at values of r lower than ξ_K. In "sintetic" TIA systems (magnetic impurities deposited over a carbon-nanotube, quantum dots connected to a quantum wire or to a confined 2D electron gas in a semiconductor heterostructure, etc.) the effective dimension is generally within 1D and 2D. The "classical" two-impurity Anderson problem corresponds to two magnetic impurities in a 3D metallic host. Here we analyze the behavior of δ and γ in the 2D and 3D cases. At this effect we only needed to evaluate C_Q. For the 3D case it results in

$$C_Q^{3D} \simeq \sin(k_F r)/k_F r \tag{65}$$

and, for the 2D case,

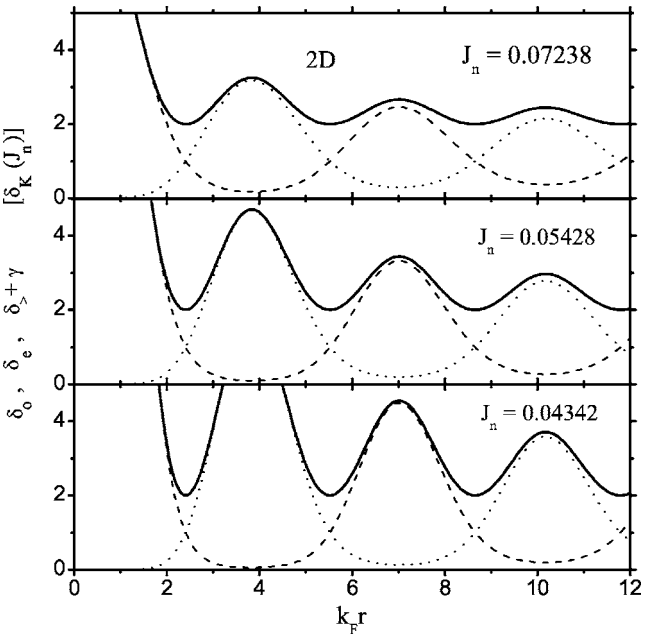

FIG. 8. Two-dimensional correlation energy gains δ_o (dashed line), δ_e (dotted line), and $\delta_> + \gamma$ (solid line) as a function of r, for values of J_n corresponding to, from top to bottom, $\delta_K = 10^{-3}D$, $10^{-4}D$, and $10^{-5}D$.

$$C_Q^{2D} \simeq \text{Bessel}J(0,k_F r), \tag{66}$$

for $r \ll \xi_K$, where the main decoherence effect is the angular one and they depend very weakly on δ. For $r \geqslant \xi_K$ C_Q decays like the power D (=1, 2, or 3) of 1 over r. The RKKY Σ_R has already the last behavior at r a fraction of λ_F.

In Fig. 8 we show three 2D cases corresponding, from top to bottom, to $J_n=0.072\,38$, $0.054\,28$, and $0.043\,43$. The corresponding values of δ_k are $0.001D$, $0.0001D$, and $0.000\,01D$ and the ones of δ_3 $[=\delta_o(0)]$, which do not depend on the dimension, are $10.0\delta_K$, $21.5\delta_K$, and $46.4\delta_K$, respectively. It can be seen that due to the angular decoherence effects, the correlation energy gains decrease more quickly, as a function of r, than in the 1D case (compare the top panel with Fig. 4). It can also be seen that the relative effect of the doublet interaction is higher the lower J_n.

In Fig. 9 we show the 3D case for the same J_n values analyzed in Fig. 8. The top panel (3D, $\delta_K=0.001D$) is the case numerically analyzed in Ref. 20 [Fig. 4(a)]. There are very minor differences; for example, the numerical simulation does not reach the δ_3 $r=0$ limit, although its authors already obtained that limit analytically. It is known that Kondo-like systems are very difficult to simulate numerically due to the logarithmic scales involved in the problem.

VI. $\langle S_L \cdot S_R \rangle$ CORRELATION

A very important observable in these systems is the impurities spin-spin correlation $\langle S_L \cdot S_R \rangle$ because of its possible application in quantum computation. It is commonly believed that this correlation is determined by the RKKY interaction. We have shown in Sec. IV A that there is a simpler process than the RKKY one that leads to an impurity-

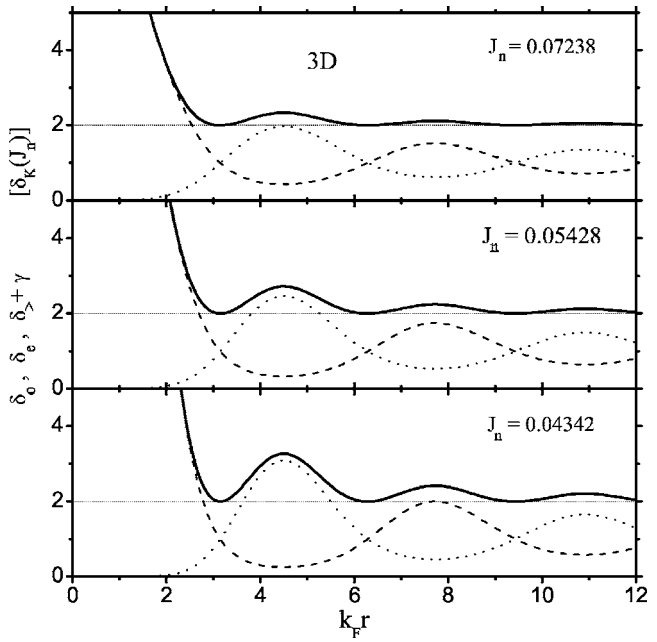

FIG. 9. Three-dimensional correlation energy gains δ_o (dashed line), δ_e (dotted line), and $\delta_> + \gamma$ (solid line) as a function of r, for the same three J_n values analyzed in the 2D case.

impurity correlation, the Kondo-doublet interaction. In Sec. IV D we have also shown that the correlation energy of the doublets is greater than the RKKY correlation energy for most of the Hamiltonian parameter space. Here we show that the Kondo-doublet interaction generates a ferromagnetic alignment of the impurity spins without resort to the RKKY mechanism.

Using for the doublet VWF's the simplest form given in Eq. (31)—i.e., without the inclusion of the higher-order RKKY effects discussed in Sec. IV D—the doublet spin-spin impurity correlation $\langle S_L \cdot S_R \rangle$ is given by

$$\frac{\langle D|S_L \cdot S_R|D\rangle}{\langle D|D\rangle} = \pm \frac{3}{4} \frac{D_Q(\delta,r)}{[2 \pm D_Q(\delta,r)]}, \tag{67}$$

where $D_Q = (\partial_\delta I_Q)/(\partial_\delta I_K)$ and the upper (lower) sign holds for the odd (even) doublet.

In Fig. 10 it can be seen that the dominant doublet favors a parallel (ferromagnetic) alignment of the impurity spins. Note that this mainly ferromagnetic response is obtained

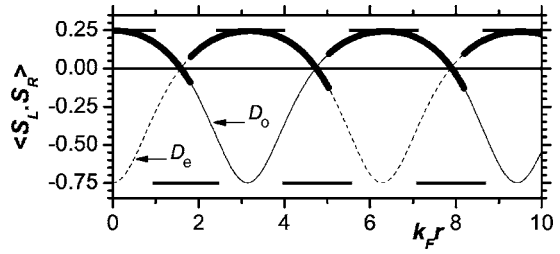

FIG. 10. Impurity-spin correlation for the doublets, without higher-order RKKY effects. The thicker section in each line is the r region dominated by the corresponding doublet. The straight segments at 1/4 (−3/4) correspond to the RKKY prediction.

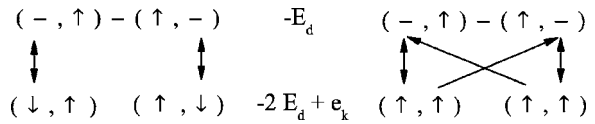

FIG. 11. First-order loop paths for the $d^\dagger_{A\uparrow}|F\rangle$ state. On the left noncorrelated $\sigma\bar{\sigma}$ channel is shown. On the right is the interference-enhanced $\sigma\sigma$ channel; the crossed arrows correspond to the inter-impurity paths.

without including the effects of the RKKY interaction in the doublet structure.

This magnetic response can be clearly understood by a closer look to the first-order interaction behind the doublets. Correlations between the impurities are the consequence of closed electron paths that involve both impurities, paths driven by H_V in configurational space. For example, the second-order RKKY-FM path starts when one electron (say, the one in the left impurity) hops to a band state k ($>k_F$) and then a second electron hops into the impurity, letting a hole q ($<k_F$) in the band. The path is closed by reversing these steps but at the other impurity. The matrix element for this loop, taking into account the mirror path, is

$$\langle\uparrow\uparrow|H_V^4|\uparrow\uparrow\rangle_{RKKY} = \mp \mathbf{v}^4 \cos(\mathbf{k}+\mathbf{q}) \cdot \mathbf{r}, \tag{68}$$

where the plus sign holds for the AF state. This correlation path produces the energy correction $\mp\Sigma_R(r)$ for the FM (AF) state, which splits the FM and AF states. We use in this section the direct orbital representation used in the unsymmetrized Hamiltonian, Eq. (1). Therefore, in the equation above, $|\uparrow\uparrow\rangle \equiv |\mathrm{FM}\uparrow\rangle \equiv d^\dagger_{L\uparrow} d^\dagger_{R\uparrow}|F\rangle$.

In this representation the vertex state of the odd doublet, $d^\dagger_{A\uparrow}|F\rangle$, is given by

$$|A_\sigma\rangle \equiv \frac{1}{\sqrt{2}}(d^\dagger_{R\sigma} \mp d^\dagger_{L\sigma})|F\rangle \equiv \frac{1}{\sqrt{2}}(|0\sigma\rangle \mp |\sigma 0\rangle), \tag{69}$$

where the plus sign is for the vertex of the even doublet, the symmetric one-electron-in-the-two-impurity $d^\dagger_{S\sigma}|F\rangle \equiv |S_\sigma\rangle$ state. The hybridization H_V connects the $|A_\uparrow\rangle$ state, by promoting an electron from below k_F to the empty impurity, with the following ones:

$$|A_{\uparrow\downarrow k}\rangle = \frac{-\mathbf{v}}{\sqrt{2}} b^\dagger_{k\uparrow}(e^{-i\mathbf{k}\cdot\mathbf{r}/2}|\uparrow\downarrow\rangle + e^{+i\mathbf{k}\cdot\mathbf{r}/2}|\downarrow\uparrow\rangle), \tag{70a}$$

$$|A_{\uparrow\uparrow k}\rangle = \frac{-\mathbf{v}}{\sqrt{2}} b^\dagger_{k\downarrow}(e^{-i\mathbf{k}\cdot\mathbf{r}/2}|\uparrow\uparrow\rangle + e^{+i\mathbf{k}\cdot\mathbf{r}/2}|\uparrow\uparrow\rangle). \tag{70b}$$

Closing the loop, as depicted in Fig. 11, the following matrix elements are obtained:

$$\langle A_\uparrow|H_V|A_{\uparrow\downarrow k}\rangle = \mathbf{v}^2, \tag{71a}$$

$$\langle A_\uparrow|H_V|A_{\uparrow\uparrow k}\rangle = \mathbf{v}^2(1 \pm \cos\mathbf{k}\cdot\mathbf{r}), \tag{71b}$$

where the minus sign corresponds to a similar path but for the $|S_\uparrow\rangle$ state. The last element, which depends on the inter-impurity distance r, determines the properties of the doublets.

As the starting state of the loop has a higher energy than the bunches of "visited" ones the energy associated with this interaction cannot be obtained by perturbative methods.[17,20] This situation, a single state connected to bunches of lower-energy states, is the hallmark of a Kondo structure, in this case the Kondo doublets that we have analyzed in the previous sections.

With the analysis above at hand, the "ferromagnetic" behavior of the impurities induced by the doublets is easy to understand. The correlated channel is the $\sigma\sigma$ one, which corresponds to a ferromagnetic arrangement of the impurities [Eqs. (70b) and (71b)]. The configurations connected via the noncorrelated $\sigma\bar{\sigma}$ channel are also mainly ferromagnetic configurations at the maxima of δ_D. See also Eqs. (33) and (60), for the dominant doublet the connectivity factor of the ferromagnetic configurations is $\sim 3(1+|C_Q|)/2$, whereas that of the antiferromagnetic ones is $\sim(1-|C_Q|)/2$. Clearly, the screening action of the hole is more effective when the impurity spins are aligned and the distance between them is near the resonant condition for the lowest-energy holes ($r \simeq n\lambda_F/2, |\cos k_F r| \simeq 1$); see Eq. (71b).

At the transition points from one doublet to the other a little negative value for $\langle S_L \cdot S_R \rangle$ is shown in Fig. 10 and then a jump to positive values. Actually, at those transition points the supersinglet has a maximum in its correlation energy ($\gamma \simeq \delta_K$) and it is formed with similar weights in both doublets; thus, an average of the response of the odd and even doublets is to be expected at those regions, given a smooth transition with a $\langle S_L \cdot S_R \rangle$ value near zero from one doublet region to the next one. In Fig. 10 the RKKY prediction is also shown, based upon $\Sigma_R(r) \gtrless 0$. Taking into account both interactions, the stronger of them determines the $\langle S_L \cdot S_R \rangle$ response of the system; for $\max(\delta_o, \delta_e) \gg |\Sigma_R|$, the response is determined by the doublet curve [Eq. (68), Fig. 10] whereas that in the opposite situation the impurity-spin correlation tends to that of the RKKY.

Now we include the RKKY effects in the doublet wave functions and thus in their $\langle S_L \cdot S_R \rangle$ correlation. Following the analysis of Sec. IV D and Appendix C, we take the variational amplitudes in the doublets to be $Z_S \sim 1/(\Delta_D - \Sigma_R + e_k)$ for the ferromagnetic configurations and $Z_A \sim 1/(\Delta_D + \Sigma_R + e_k)$ for the antiferromagnetic ones, where $\Delta_D = |\Sigma_R| + \delta_D^{\Sigma}$ as evaluated in the RKKY-doublet section. Thus, including RKKY effects, the impurity-spin correlation of the odd doublet is given by

$$\langle S_L \cdot S_R \rangle = \frac{\frac{1}{4} 3 J_K^S (1 + D_Q^S) - \frac{3}{4} J_K^A (1 - D_Q^A)}{3 J_K^S (1 + D_Q^S) + J_K^A (1 - D_Q^A)}, \qquad (72)$$

where $D_Q^{S(A)} = D_Q(\Delta_{D_o} \mp \Sigma_R, r)$ and

$$J_K^{S(A)} = \frac{2}{n_o N_c} \sum_k \frac{1}{(\Delta_{D_o} \mp \Sigma_R + e_k)^2}, \qquad (73)$$

and for the even doublet the change $D_Q \mapsto -D_Q$ must be done. The *supra* $S(A)$ terms come from the contribution of the ferromagnetic (antiferromagnetic) configurations of the doublet. Equation (72) reduces to the previous equation (67) for $\delta_D(r) \gg |\Sigma_R(r)|$. Equation (72) reflects the changes in the energies of the FM and AF impurity configurations produced by the RKKY interaction. Thus in a RKKY-FM region the relative variational amplitude of the ferromagnetic configurations is greater than the one of the antiferromagnetic ones, $1/(\delta_D + e_k) \gg 1/(2\Sigma_R + \delta_D + e_k)$, given a ferromagnetic like $\langle S_L \cdot S_R \rangle$ correlation. The opposite is true in a RKKY-AF region. Note instead that the ferromagnetic response induced by the Kondo-doublet interaction depends on the interference-enhanced matrix elements, the $(1 \pm D_Q)$ factors in Eq. (72), not in the difference of energy between the FM and AF impurity configurations.

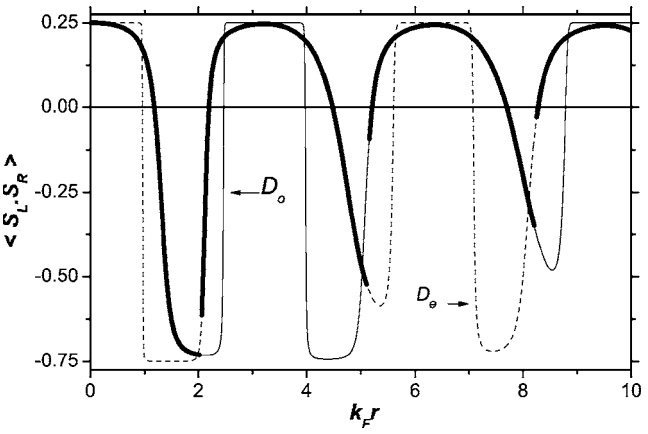

FIG. 12. Impurity-spin correlation for the doublets, RKKY effects included. The thicker section in each line is the r region dominated by the corresponding doublet. The dominated doublet (thin lines) closely follows the RKKY prediction.

In Fig. 12 we plot the $\langle S_L \cdot S_R \rangle$ response of the doublets, RKKY effects included, for the same 1D case plotted in Fig. 10. There is an abrupt change in the response of the dominated doublet (thin lines): as $\delta_<$ is exponentially small (see Fig. 3) the RKKY effects determine the response of the dominated doublet. Thus the thin lines closely follow the RKKY response, jumping from $1/4$ to $-3/4$ (and back) at the $\Sigma_R(r)=0$ points. Instead, the dominant doublet response (thick sections) is little modified by the RKKY interaction except at the extreme RKKY-AF point at $k_F r \simeq 2$, where $|\Sigma_R(r)| > \delta_>(r)$ and thus the RKKY-AF behavior dominates. As discussed in Fig. 7 this point corresponds to a maximum of the antiferromagnetic RKKY interaction and to a minimum of the Kondo-doublet interaction ($C_Q \simeq 0$). Note also that the ferromagnetic response induced by the Kondo-doublet interaction persists well into the RKKY-AF region.

For the supersinglet, Eq. (38), the $\langle S_L \cdot S_R \rangle$ correlation is approximately given by a weighted average of the dominant and dominated doublet response. The weighting factors are proportional to the average of the square of the corresponding amplitudes in the supersinglet VWF, $Z_O(k) \sim 1/(\gamma + e_k)$ and $Z_E(k) \sim 1/(\gamma + \Delta_\delta + e_k)$, respectively (in the $\delta_o > \delta_e$ case), which turn out to be proportional to $1/\gamma$ and $1/(\gamma + \Delta_\delta)$.

In Fig. 13 we plot the supersinglet and doublet $\langle S_L \cdot S_R \rangle$ correlations for a 3D and a 2D case (without RKKY effects). Note that in both the 2D and 3D cases the ferromagnetic correlation induced by the doublets is present for interimpurity distances of several times λ_F.

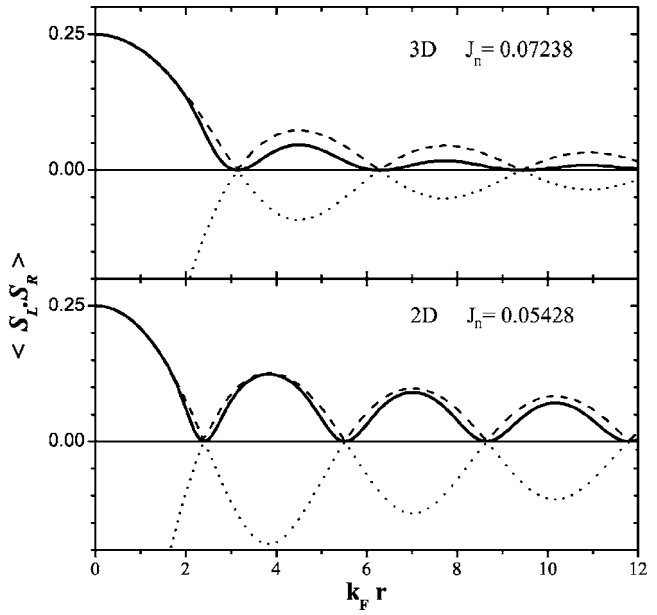

FIG. 13. $\langle S_L \cdot S_R \rangle$ for the supersinglet (solid line), the dominant doublet (dashed line), and the dominated doublet (dotted line) as a function of the distance between the impurities. The upper panel is for a 3D case and the lower one for a 2D case.

VII. CONCLUSIONS

We have presented a simple and complete analysis of the two-Anderson-impurity system. The variational wave functions we use to analyze the problem are generated in each subspace of the Hamiltonian starting with the simplest configuration and applying to it the hybridization terms—i.e., the nondiagonal part of the Hamiltonian. The configurations so generated are grouped together with a variational amplitude function according to their internal symmetry. This step is repeated as many times as needed to bring out the physics of the state. One step is necessary for the doublet states, two for the supersinglet, one to connect the doublets through the Fermi-sea state and one to retain the internal structure of the doublets; two more are included in Appendix C to show how the doublets are affected by the RKKY interaction. In this aspect, the technical method we use is in fact an analytical Lanczos method, to some point similar to the one used in Ref. 25, but with variational functions as amplitude coefficients. Such variational functions are found by the classical method—i.e., Euler-Lagrange minimization of the energy functional, which is also evaluated analytically.

This method can be also applied to the case of M impurities, especially if the symmetry group of the impurity arrangement is contained in the symmetry group of the metallic host. In such a case M steps will be needed in the variational M supersinglet to arrive at the states with M electrons in the impurities, starting from the $|F\rangle$ vacuum state. But our conjecture is that, for a given set of system parameters, the physical relevant state is the M-multiplet constructed by forming a Kondo singlet in the higher effective hybridization channel and filling the other effective impurities with one electron, as we do in Sec. III B, to form our first approximation to the odd doublet. Starting from this M-multiplet and going down, step after step, towards the $|F\rangle$ state, each successive step will introduce a exponentially small correction to the M-multiplet energy, as γ correct δ_D in the case we analyzed, Sec. III C. Other impurity configurations, like three in a row, are also of interest. The equations of the three-in-a-row case can be easily obtained from the present study by adding an impurity at the origin. In Appendix B we outline this case and show that for certain values of r the effective hybridization is very large in the active channel. A full analysis will be presented elsewhere.

The TIA Kondo doublet states generate a ferromagnetic-impurity–spin correlation, without resort to the RKKY interaction. The correlation energy gain of these doublets, which is driven by a first-order direct coherence effect of the hybridization, exceeds that of the second-order RKKY interaction for most of the Hamiltonian parameter space (J_n, r). These properties put the states we found well in the experimentally accessible range for quantum dot systems built on semiconductor devices,[26] where most of the relevant parameters can be controlled by gate voltages.

A milestone of the two-magnetic-impurity problem is the renormalization group analysis of Ref. 9. This work was carried out in the symmetrized basis too, but the r dependence of the effective hybridization was treated in a crude fashion, just taking its value at $k=k_F$, the relevance of the increased value of the effective hybridization being missed. Nevertheless, the two energy scales found in that work can be traced to be the γ and δ_D correlation energy gains of the supersinglet and doublets. Their coupling parameters J_o and J_e are related to the square of our effective hybridization terms—i.e., $\sim[1 \pm C_Q(\delta, r)]$—and their "Kondo temperatures" $T_K(J_e)$ and $T_K(J_o)$ to our δ_D and γ, which are not the Kondo energies corresponding to J_e and J_o but Eqs. (35) and (50). We show that their relative relevance depends on the value of $C_Q(\delta_K, r)$; for $C_Q(\delta_K) \simeq 0$, both are equally relevant and both tend to δ_K. Our results are also in perfect accord with the VWF numerical analysis of Andreani and Beck.[20]

Summarizing, our results confirm the general picture of the system behavior already known from numerical simulations, but thanks to our explicit VWF that we analytically solve in the different subspaces of the TIA, they also point out important differences with the usual interpretation of that numerical data. The main interaction between the impurities, contrary to the general belief, is not generated by the RKKY process but by the interference-enhanced hybridization that generates the Kondo-doublet states. The strength of this Kondo-doublet interaction depends on the one-hole quantum interference factor $C_Q(r)$.

For interimpurity distances r around the maxima of $|C_Q(r)|$ a two-stage Kondo screening takes place. It is a correlated quenching of the total spin of the system, not the successive "one-impurity" Kondo screening of the odd and even hybridization channels.[9,15] It also generates a strong ferromagnetic correlation between the impurity spins because the interference effects increase the weight of the ferromagneticlike impurity configurations in the dominant doublet. The ferromagnetic r regions of the RKKY interaction are comprised in these zones. For low values of both the coupling constant J_n and r the RKKY interaction is strongest

than the Kondo-doublet interaction ($\Sigma_R > \delta_> \gg \delta_K$). However, this has little effect in the structure of the TIA Kondo states because the ferromagneticlike impurity configurations are already their main component. In a "temperature scheme"[15] this situation ($\Sigma_R > \delta_>$) generates the intermediate triplet spin-1 phase between the high-temperature uncorrelated impurity spin phase and the doublet spin-1/2 region.

For r near the zeros of $C_Q(r)$ there is no enhancement of the Kondo-doublet energies ($\delta_o, \delta_e \simeq \delta_K$) and the system behavior tends to that of two uncorrelated Kondo impurities. The maxima of the antiferromagnetic RKKY coincide with these points. If $-\Sigma_R > \delta_K$, the antiferromagnetic like impurity configurations dominate the structure and response of the TIA Kondo states, but between the limits of our calculation, there is not a true quantum phase transition from the Kondo supersinglet to an AF singlet.[14]

We provide detailed formulas for the evaluation, in all dimensions and for any value of J_n and r, of the Kondo energies of the TIA Hamiltonian. We provide also explicit formulas for the evaluation of the impurity spin-spin correlation in a given experimental situation. As we provide the explicit VWF of the involved states, other correlations can also be easily evaluated.

ACKNOWLEDGMENTS

I am grateful to Blas Alascio, Carlos Balseiro, Eduardo Jagla, César Proetto, and María Dolóres Núñez Regueiro for useful talks. This research was partially financed by CONICET (Argentina) under Grant No. PIP 02753/00.

APPENDIX A: M-CHANNEL SINGLET

Given that for an arrangement of M magnetic impurities is always possible to construct an M-channel singlet, the first step of the M-supersinglet, it is worthwhile to show that, although $\delta_{2M} \gg \delta_K$, its total energy, $E_M = -Ed - \delta_{2M}$ is always greater than the energy of M decoupled Kondo singlets, $E_{dc} = M(-E_d - \delta_K)$. Therefore, Eq. (5), we must show that

$$-E_d - \delta_{2M} = -2M\mathbf{v}^2 \sum_q \frac{1}{\delta_{2M} + e_q} \tag{A1}$$

is always greater than

$$-M(E_d + \delta_K) = -M2\mathbf{v}^2 \sum_q \frac{1}{\delta_K + e_q}. \tag{A2}$$

Comparing the sums term to term, we see that in each of them $1/\delta_K + e_q > 1/\delta_{2M} + e_q$ for $\delta_{2M} > \delta_K$. Thus $E_M > E_{dc}$ independently of the $D, E_d \gg \delta$ usual approximation and for any distribution of the conduction band hole states (q). In particular, this applies for $M=2$, Sec. III A.

APPENDIX B: THREE-IN-A-ROW CASE

For the three-in-a-row impurity case, two as analyzed in this paper plus one at the origin, one can take as normal modes of the impurities the following symmetrized combinations of the impurity orbitals:

$$A = (-1/\sqrt{2}, 0, 1/\sqrt{2}), \tag{B1}$$

$$S_1 = (1/\sqrt{3}, 1/\sqrt{3}, 1/\sqrt{3}), \tag{B2}$$

$$S_2 = (1/\sqrt{6}, -2/\sqrt{6}, 1/\sqrt{6}). \tag{B3}$$

In each of these combinations the first coefficient is the amplitude of the normal mode at the left impurity, the second coefficient is the amplitude at the impurity at the origin, and the third coefficient is the one corresponding to the right impurity. The hybridization matrix elements, with the symmetric ($\sqrt{2}\cos k_x x$) and antisymmetric ($i\sqrt{2}\sin k_x x$) conduction band orbitals, are

$$V_A = \langle d_A | H_{hyb} | c_{Ak} \rangle = 2i\mathbf{v} \sin k_x r/2, \tag{B4}$$

for the combination A, as before [see Eq. (8)], and

$$V_{S_1} = \langle d_{S1} | H_{hyb} | c_{Sk} \rangle = \sqrt{\frac{2}{3}}\mathbf{v}(1 + 2\cos k_x r/2), \tag{B5}$$

$$V_{S_2} = \langle d_{S2} | H_{hyb} | c_{Sk} \rangle = \sqrt{\frac{2}{6}}\mathbf{v}(-2 + 2\cos k_x r/2), \tag{B6}$$

for the symmetric combinations S. Therefore for $r = 2\lambda_F$ one has $\{V_A \simeq 0, V_{S_1} \simeq \sqrt{6}\mathbf{v}, V_{S_2} \simeq 0\}$ and a strong 3-multiplet can be proposed, formed upon a Kondo singlet in the S_1 impurity plus one electron in each one of the other impurity normal modes.

APPENDIX C: THE ODD DOUBLET IN AN EXTREME RKKY-AF REGION

In order to show the validity of Eq. (60) to analyze the RKKY effects in our doublets, we present here a partial deduction of it. Assuming we are in an extreme RKKY-AF region, we can drop the contribution of the FM-like impurity configurations to the odd doublet. Therefore we start with

$$|\mathbf{D}_{o\uparrow}\rangle = d^\dagger_{A\uparrow}|F\rangle + i\sum_k Z_A(k) A_k b^\dagger_{Ak\uparrow}|\mathrm{AF}\rangle. \tag{C1}$$

Applying H_V to the Z_A configurations, one electron is removed from the impurities and transferred to the band states. Given the structure of $|\mathrm{AF}\rangle$ there are four possibilities, two corresponding to the transfer of a symmetric electron (with a probability amplitude proportional to S_q) and the other two corresponding to the transfer of an antisymmetric electron ($\sim iA_q$); therefore, the following states are added to the VWF:

$$+\sum_{k,q} A_k b^\dagger_{Ak\uparrow}\{iS_q[Y_1(k,q)c^\dagger_{Sq\downarrow}d^\dagger_{S\uparrow}|F\rangle - Y_2(k,q)c^\dagger_{Sq\uparrow}d^\dagger_{S\downarrow}|F\rangle]$$
$$- A_q[Y_3(k,q)c^\dagger_{Aq\downarrow}d^\dagger_{A\uparrow}|F\rangle - Y_4(k,q)c^\dagger_{Aq\uparrow}d^\dagger_{A\downarrow}|F\rangle]\}, \tag{C2}$$

applying again H_V, a big set of new configurations is generated. The ones with one electron in each impurity are the ones of lower energy, and of these, in order to maintain this presentation as simple as possible, we include here only the ones that contribute to the RKKY interaction:

$$+\sum_{k,q,p} A_k b^\dagger_{Ak\uparrow}\{-S_q A_p[X_1(k,q,p)b^\dagger_{Ap\downarrow}c^\dagger_{Sq\downarrow}|\mathrm{FM}\uparrow\rangle - X_2(k,q,p)b^\dagger_{Ap\uparrow}c^\dagger_{Sq\uparrow}|\mathrm{FM}\downarrow\rangle] + A_q S_p[X_3(k,q,p)b^\dagger_{Sp\downarrow}c^\dagger_{Aq\downarrow}|\mathrm{FM}\uparrow\rangle - X_4(k,q,p)b^\dagger_{Sp\uparrow}c^\dagger_{Aq\uparrow}|\mathrm{FM}\downarrow\rangle]\}. \quad \text{(C3)}$$

The discarded ones, with their impurity part in a $|\mathrm{FM0}\rangle$ or a $|\mathrm{AF}\rangle$ state, contribute only to the "one-impurity" correction. They were included in Sec. IV C. The energy of the doublet is given by

$$E_D = \langle \mathbf{D}_{o\uparrow}|H|\mathbf{D}_{o\uparrow}\rangle / \langle \mathbf{D}_{o\uparrow}|\mathbf{D}_{o\uparrow}\rangle. \quad \text{(C4)}$$

The variation of Eq. (C4) with respect to $Z_A(k),\ldots,X_4(k,q,p)$ gives nine coupled equations. These equations can be used to reduce Eq. (C4) to the form

$$E_D = -E_d + 2\mathbf{v}\sum_k \sin\left(\frac{k_x r}{2}\right)^2 Z_A(k). \quad \text{(C5)}$$

The variational equations are solved in a progressive way, starting with the higher-order amplitude factors

$$X_1(k,q,p) = -2\mathbf{v}Y_1(k,q)/D_X(k,q,p),$$

$$X_2(k,q,p) = -\mathbf{v}[Y_2(k,q) - Y_2(p,q)]/D_X(k,q,p),$$

$$X_3(k,q,p) = -2\mathbf{v}Y_3(k,q)/D_X(k,q,p),$$

$$X_4(k,q,p) = -2\mathbf{v}Y_4(k,q)/D_X(k,q,p), \quad \text{(C6)}$$

where

$$D_X(k,q,p) = -E_D - 2E_d + e_k + e_q + e_p. \quad \text{(C7)}$$

Using the above results, the Y_i factors are found:

$$Y_1(k,q) = -2\mathbf{v}Z_A(k)/D_{YS}(k,q),$$

$$Y_2(k,q) = -2\mathbf{v}Z_A(k)/D_{YS}(k,q) + 4\mathbf{v}^2\sum_p [A_p^2 Y_2(p,q)/D_X(k,q,p)]D_{YS}(k,q),$$

$$Y_3(k,q) = -2\mathbf{v}Z_A(k)/D_{YC}(k,q),$$

$$Y_4(k,q) = -2\mathbf{v}Z_A(k)/D_{YC}(k,q), \quad \text{(C8)}$$

where

$$D_{YS}(k,q) = -E_D - E_d + e_k + e_q - 4\mathbf{v}^2\sum_p A_p^2/D_X(k,q,p),$$

$$D_{YC}(k,q) = -E_D - E_d + e_k + e_q - 4\mathbf{v}^2\sum_p S_p^2/D_X(k,q,p). \quad \text{(C9)}$$

The Y_i factors carry the RKKY effects into the variational equation obtained for Z_A, which is

$$(E_D + 2E_d - e_k)Z_A(k) = \mathbf{v} + \mathbf{v}\sum_q \left\{\cos^2\left(\frac{q_x r}{2}\right)[Y_1(k,q) + Y_2(k,q)] + \sin^2\left(\frac{q_x r}{2}\right)\times[Y_3(k,q) + Y_4(k,q)]\right\}. \quad \text{(C10)}$$

This is a self-consistent equation, the Y_i factors depending themselves on Z_A. In order to solve it and to obtain the standard expression for the RKKY contribution, the Y_i factors must be expanded in powers of $\mathbf{v}$, as already done in Sec. IV C:

$$Y_1(k,q) = Z_A(k)[\mathbf{v}y_0(k,q) + \mathbf{v}^3 y_{2S}(k,q)],$$

$$Y_2(k,q) = Y_1(k,q) + \mathbf{v}^3 y_{2X}(k,q),$$

$$Y_3(k,q) = Z_A(k)[\mathbf{v}y_0(k,q) + \mathbf{v}^3 y_{2C}(k,q)],$$

$$Y_4(k,q) = Y_3(k,q), \quad \text{(C11)}$$

where, with $D_Y(k,q) = -E_D - E_d + e_k + e_q$,

$$y_0(k,q) = -2/D_Y(k,q),$$

$$y_{2S}(k,q) = \frac{-8}{D_Y^2(k,q)}\sum_p \sin^2\left(\frac{p_x r}{2}\right) \Big/ D_X(k,q,p),$$

$$y_{2C}(k,q) = \frac{-8}{D_Y^2(k,q)}\sum_p \cos^2\left(\frac{p_x r}{2}\right) \Big/ D_X(k,q,p),$$

$$y_{2X}(k,q) = \frac{-8}{D_Y(k,q)}\sum_p \frac{Z_A(p)\sin^2(p_x r/2)}{D_Y(q,p)D_X(k,q,p)}. \quad \text{(C12)}$$

Using the above equations in the variational equation for $Z_A(k)$,

$$Z_A(k) = \frac{-\mathbf{v}(1-\mathbf{v}^3\Gamma_Z)}{-E_D - 2E_d + e_k - \Sigma_Z}, \quad \text{(C13)}$$

is obtained, where

$$\Gamma_Z = 8\sum_{q,p} \frac{Z_A(p)\sin^2(p_x r/2)\cos^2(q_x r/2)}{D_Y(k,q)D_Y(q,p)D_X(k,q,p)},$$

$$\Sigma_Z = 4\mathbf{v}^2\sum_q \frac{1}{D_Y(k,q)} + 8\mathbf{v}^4\sum_{q,p} \frac{1-\cos(q_x r)\cos(p_x r)}{D_Y^2(k,q)D_X(k,q,p)} \simeq 2\Sigma_{01} + \Sigma_{02} - \Sigma_R(r). \quad \text{(C14)}$$

Both Γ_Z and Σ_Z are very weakly dependent on e_k; in fact, it is a common practice to substitute factors of the kind $1/(E_d+e_k)$ by $1/E_d$ in the available calculus of the RKKY interaction, a notable exception being Ref. 27. In any case, such an approximation overestimates the RKKY effects. Σ_{0i} is the order-J_n^i "one-impurity" correction. Γ_Z can be evaluated by substituting $Z_A(p)$ by its first-order approximation $\mathbf{v}/(E_D+2E_d-e_p)$; Γ_Z gives a J_n^2 correction to the "connectiv-

ity" factor of the AF configurations involved in the odd doublet. In the equations above the sums over k,p (q) are over "symmetrized" hole (electron) excitations. From Eqs. (C5), (C13), and (C14) the last term on the right-hand side of Eq. (60) immediately follows.

We have analyzed the general situation—i.e., including the Z_S FM-like configurations in the doublet (and the corresponding secondary configurations)—in order to fully certify Eq. (60). Our "second-quantization" Mathematica package does the calculations needed for Eq. (C4) on the fly; a primitive version of this package was used in Refs. 28 and 29. To bring those equations to ink, instead, will take a considerable amount of pages and time. The general procedure is similar to the one we outlined here for the extreme RKKY-AF case.

[1] B. Coqblin and J. R. Schieffer, Phys. Rev. **185**, 847 (1969).
[2] N. J. Craig, J. M. Taylor, E. A. Lester, C. M. Marcus, M. P. Hanson, and A. C. Gossard, Science **304**, 565 (2004).
[3] P. Simon, Phys. Rev. B **71**, 155319 (2005).
[4] D. Goldhaber-Gordon, H. Shtrikman, D. Mahalu, D. Abusch-Magder, U. Meirav, and M. A. Kastner, Nature (London) **391**, 156 (1998).
[5] C. R. Proetto and A. López, Phys. Rev. B **25**, 7037 (1982).
[6] S. Galkin, C. A. Balseiro, and M. Avignon, Eur. Phys. J. B **38**, 519 (2004).
[7] R. Allub, Phys. Rev. B **67**, 144416 (2003).
[8] C. Jayaprakash, H. R. Krishna-murthy, and J. W. Wilkins, J. Appl. Phys. **53**, 2142 (1982).
[9] B. A. Jones and C. M. Varma, Phys. Rev. Lett. **58**, 843 (1987).
[10] C. Jayaprakash, H. R. Krishna-murthy, and J. W. Wilkins, Phys. Rev. Lett. **47**, 737 (1981).
[11] B. A. Jones, C. M. Varma, and J. W. Wilkins, Phys. Rev. Lett. **61**, 125 (1988).
[12] K. Ingersent, B. A. Jones, and J. W. Wilkins, Phys. Rev. Lett. **69**, 2594 (1992).
[13] J. B. Silva, W. L. C. Lima, W. C. Oliveira, J. L. N. Mello, L. N. Oliveira, and J. W. Wilkins, Phys. Rev. Lett. **76**, 275 (1996).
[14] B. A. Jones, Ph.D. thesis, Cornell University, 1987.
[15] R. M. Fye and J. E. Hirsch, Phys. Rev. B **40**, 4780 (1989).
[16] P. Schlottmann, Phys. Rev. Lett. **80**, 4975 (1998).
[17] C. M. Varma and Y. Yafet, Phys. Rev. B **13**, 2950 (1976).
[18] T. Saso, Phys. Rev. B **44**, 450 (1991).
[19] T. Saso and H. Kato, Prog. Theor. Phys. **87**, 331 (1992).
[20] L. C. Andreani and H. Beck, Phys. Rev. B **48**, 7322 (1993).
[21] P. Simon, R. López, and Y. Oreg, Phys. Rev. Lett. **94**, 086602 (2005).
[22] M. G. Vavilov and L. I. Glazman, Phys. Rev. Lett. **94**, 086805 (2005).
[23] V. I. Litvinov and V. K. Dugaev, Phys. Rev. B **58**, 3584 (1998).
[24] J. Simonin, cond-mat/0503163 (unpublished).
[25] J. D. Mancini and D. C. Mattis, Phys. Rev. B **28**, 6061 (1983).
[26] H. Tamura, K. Shiraishi, and H. Takayanagi, Jpn. J. Appl. Phys., Part 2 **43**, L691 (2004).
[27] C. R. Proetto, Ph.D. thesis, Instituto Balseiro, 1985.
[28] A. A. Aligia, M. E. Simon, and C. D. Batista, Phys. Rev. B **49**, 13061 (1994).
[29] J. Simonin and R. Allub, Phys. Rev. Lett. **74**, 466 (1995).